

Alma Mater Studiorum Università di Bologna
Archivio istituzionale della ricerca

Mediterranean Sea large-scale, low-frequency ocean variability and water mass formation rates from 1987 to 2007: a retrospective analysis.

This is the final peer-reviewed author's accepted manuscript (postprint) of the following publication:

Published Version:

Pinardi N., Zavatarelli M., Adani M., Coppini G., Fratianni C., Oddo P., et al. (2015). Mediterranean Sea large-scale, low-frequency ocean variability and water mass formation rates from 1987 to 2007: a retrospective analysis. PROGRESS IN OCEANOGRAPHY, 132, 318-332 [10.1016/j.pocean.2013.11.003].

Availability:

This version is available at: <https://hdl.handle.net/11585/133955> since: 2016-01-11

Published:

DOI: <http://doi.org/10.1016/j.pocean.2013.11.003>

Terms of use:

Some rights reserved. The terms and conditions for the reuse of this version of the manuscript are specified in the publishing policy. For all terms of use and more information see the publisher's website.

This item was downloaded from IRIS Università di Bologna (<https://cris.unibo.it/>).
When citing, please refer to the published version.

(Article begins on next page)

This is the final peer-reviewed accepted manuscript of:

Nadia Pinardi, Marco Zavatarelli, Mario Adani, Giovanni Coppini, Claudia Fratianni, Paolo Oddo, Simona Simoncelli, Marina Tonani, Vladislav Lyubartsev, Srdjan Dobricic, Antonio Bonaduce, Mediterranean Sea large-scale low-frequency ocean variability and water mass formation rates from 1987 to 2007: A retrospective analysis. Progress in Oceanography, 2015, Volume 132, Pages 318-332.

The final published version is available at:
<https://doi.org/10.1016/j.pocean.2013.11.003>

Rights / License:

The terms and conditions for the reuse of this version of the manuscript are specified in the publishing policy. For all terms of use and more information see the publisher's website.

This item was downloaded from IRIS Università di Bologna (<https://cris.unibo.it/>)

When citing, please refer to the published version.

**Mediterranean Sea large-scale low-frequency ocean variability
and water mass formation rates from 1987 to 2007: a
retrospective analysis**

Nadia Pinardi*, Marco Zavatarelli

Department of Physics, University of Bologna, Italy

Mario Adani, Giovanni Coppini, Claudia Fratianni,

Paolo Oddo, Simona Simoncelli, Marina Tonani

Istituto Nazionale di Geofisica e Vulcanologia, Sezione di Bologna, Italy ,

National Group of Operational Oceanography

Vladislav Lyubartsev, Srdjan Dobricic, Antonio Bonaduce

Centro EuroMediterraneo per i Cambiamenti Climatici, Bologna, Italy

* *Corresponding author address:* Nadia Pinardi, Department of Physics, University of Bologna, Italy

E-mail: n.pinardi@sincem.unibo.it

ABSTRACT

We describe a synthesis of the Mediterranean Sea circulation structure and dynamics from a 23-year-long reanalysis of the ocean circulation carried out by Adani et al. (2011). This mesoscale permitting dynamical reconstruction of past ocean variability in the Mediterranean Sea allows the study of the time-mean circulation and its low frequency, decadal, components. It is found that the time-mean circulation is composed of boundary and open ocean intensified jets at the border of cyclonic and anticyclonic gyres. The large scale basin circulation is generally characterized in the northern regions by cyclonic gyres and in its southern parts by anticyclonic gyres and eddy-dominated flow fields, with the exception of the Tyrrhenian and the northern Ionian Sea. The time-mean Tyrrhenian Sea circulation is dominated by cyclonic gyres of different intensity and intermittency. The northern Ionian Sea circulation, however, reverses in sign in two ten-year periods, the first in 1987-1996 and the second in 1997-2006, which is here called the Northern Ionian reversal phenomenon. This reversal is provoked by the excursion of the Atlantic-Ionian Stream from the middle to the northern parts of the basin. The decadal variability of other parts of the basin is characterized by changes in strength of the basin scale structures instead. The water mass formation rates and variability are dominated by event-like periods where the intermediate and deep waters are formed for 2-3 years at higher rates. The largest deep water formation events of the past 23 years occurred separately in the western and eastern Mediterranean basin: the first coincided with the Eastern Mediterranean Transient (Roether et al. 1996) and the second with the western Mediterranean deep water formation event in 2005-2006 (Smith et al. 2008). A new schematic of the basin-scale circulation is formulated and commented.

1. Introduction

The Mediterranean Sea is a well-known anti-estuarine semi-enclosed sea that can be subdivided into two anti-estuarine sub-basins, the western and eastern Mediterranean, respectively west and east of the Sicily Strait sill (see Fig. 1). The negative heat and fresh water budgets correspond to a net loss of about 5 Wm^{-2} and 0.7 my^{-1} and are balanced by entering heat and water from the Strait of Gibraltar. This steady-state balance is achieved at multidecadal time scales, while at seasonal and interannual time scales heat can be stored and partially lost by single wintertime large evaporation events (Garrett et al. 1993; Pettenuzzo et al. 2010). The river runoff from the basin catchment is only about 10% of the net water flux into the sea (Struglia et al. 2004) but its decrease in past decades due to water usage in agriculture is probably the largest human impact on the Mediterranean Sea ecosystem (Ludwig et al. 2009).

Mediterranean Sea circulation is forced, like that of all the major ocean areas of the world, by the combined effects of wind stress and buoyancy fluxes. In the past, idealized and coarse-resolution studies have indicated that the basin circulation has a double gyre structure (Pinardi and Navarra 1993; Pinardi and Masetti 2000; Molcard et al. 2002) due to westerly winds crossing the basin from November to June (Korres et al. 2000; Castellari et al. 1998). Due to the wind stress curl sign, the northern areas are characterized by cyclonic circulations while the southern areas by anticyclonic motion. As for the North Atlantic, the cyclonic northern gyres are also forced by deep and intermediate water formation processes while the southern gyres store intermediate-mode waters which compose the permanent thermocline of the basin.

As a mid-latitude basin, the Mediterranean Sea has a large water mass formation cycle which is impacted by the entering Atlantic Water (AW) from the Strait of Gibraltar. The fresher AW characterizes the upper 50 to 100 m layer which overlies the Levantine Intermediate Water (LIW) formed in the Levantine basin (Lascaratos et al. 1993). The deep water masses are distinct between the western and eastern parts of the basin since the Sicily Strait

sill has a maximum depth of 500 m. The Western Mediterranean Deep Waters (WMDW) and the Eastern Mediterranean Deep Waters (EMDW) are formed in the Gulf of Lion area and the southern Adriatic Sea respectively (see Fig. 1), but deep waters can also form in the Rhodes gyre (Levantine Deep Water, LDW, Gertman et al. (1994)) and in the Sea of Crete (CDW, Tsimplis et al. (1999)). In the late eighties and early nineties a large climatic event known as the Eastern Mediterranean Transient (EMT, Roether et al. (1996)) showed for the first time the contribution of the Aegean Sea to the Eastern Mediterranean deep waters.

The Mediterranean Sea has also been found to have a dominant mesoscale circulation component (Robinson et al. 1987; Ayoub et al. 1998), similar to the world ocean, but also specific to this basin. Parts of the eddy field is constituted by semi-permanent eddies that due to this specific persistency in time may be also called gyres. This is the case of the Ierapetra and Pelops gyres described in several papers as recurrent gyres (Larnicol et al. 2002) with a spatial scale of the order of 10-12 times the local Rossby radius of deformation (Hecht et al. 1988) or about 120 *km* in diameter. The time persistency of this specific eddy field is still an unresolved problem but probably three factors contribute: the non-linear dynamical balances, the specific atmospheric forcing and the bathymetry. The nonlinear versus Rossby wave linear dynamics balance is synthesized in the beta Rossby number:

$$\beta = \frac{\beta_0 L^2}{U}$$

where L is the eddy scale, U the velocity scale and β_0 is the latitudinal gradient of the Coriolis parameter. This nondimensional number is the ratio between the planetary and relative vorticity advection (Pedlosky 1979). For the Mediterranean, $U = 0,01 \text{ ms}^{-1}$, $L = 10 \text{ km}$ while for the North Atlantic $U = 0,1 \text{ ms}^{-1}$, $L = 100 \text{ km}$ with $\beta_0 = 10^{-11} \text{ m}^{-1}\text{s}^{-1}$ for both, resulting in a beta Rossby number of 0.2 and 2 for the Mediterranean and North Atlantic respectively. This shows that stronger nonlinear dynamical balances may be expected in the Mediterranean Sea, driving large inverse energy cascades (Rhines 1979) and inhibiting planetary wave dynamics, thus enhancing the persistency of eddies in the basin.

The general objectives of the present study are: 1) to assess for the first time the large-scale time-mean circulation structure of Mediterranean Sea; 2) to quantify the low-frequency time variability of the circulation; 3) to describe the major water mass formation events and explore the relationship between them.

The paper is organized as follows: Section 2 illustrates the reanalysis data set; Section 3 shows the mean circulation; Section 4 the decadal mean circulation structure; Section 5 the barotropic wind driven circulation and its decadal variability; Section 6 synthesizes the water mass formation process variability. A discussion section concludes the paper.

2. The reanalysis data set

The quality of, and the methodology used to produce, the first high-resolution reanalysis for the Mediterranean Sea is described in detail in Adani et al. (2011). In this section we will only overview some important methodological aspects and we will mention some overall quality indices.

The Mediterranean Sea reanalysis has been produced using the historical profiles from the MedAtlas data set (Maillard et al. 2005) and the operational observational network of MFS (Pinardi and Coppini 2010). The historical data set consists of MBT, BT, CTD and XBT data from 1912 to approximately 2000. The operational MFS network, on the other hand, consists of real-time satellite and in-situ data, from 1992 and 1999 respectively, to today. The in-situ data are composed of temperature vertical profiles down to 700 metres provided by a ship-of-opportunity programme (Manzella et al. 2007) and temperature and salinity profiles down to 700 and 2000 metres implemented by the Medargo program (Poulain et al. 2007). The real-time satellite measurements consist of along-track Sea Level Anomaly (SLA) from altimetry (Pinardi et al. 2003). In addition, a reprocessed five-day mean Sea Surface Temperature (SST) product from 1985 to 2005 (Marullo et al. 2007) has been considered, while for the last two years a daily real-time SST product (Buongiorno Nardelli et al. 2003)

has been used.

The numerical model used for the reanalysis is described in Adani et al. (2011) and has 71 non-uniform z-coordinate levels and a horizontal resolution of $1/16^\circ \times 1/16^\circ$. The domain covers the entire Mediterranean Sea and a portion of the Atlantic Ocean, where an Atlantic box is designed to parameterize coupling between the Mediterranean and the Atlantic. The model is forced by European Centre for Medium-Range Weather Forecasts (ECMWF) surface fields using interactive air-sea physics (Pinardi et al. 2003; Tonani et al. 2009). The initial condition for January 1, 1985 is taken from the January climatology of the Medatlas data set (Rixen et al. 2004) and atmospheric realistic forcing is imposed from the beginning of the reanalysis without any relaxation to the climatology itself.

All the satellite and in-situ data are assimilated using a 3D variational assimilation scheme, OceanVar (Dobricic and Pinardi 2008), that produces ocean daily reanalyses. Both the historical and in-situ data are only used to a depth of 1000 metres, as we assume knowledge of the background error covariance matrix only to that depth. For more details see Dobricic et al. (2007). The SST is used as a surface heat flux correction term. The quality of the reanalysis has been evaluated in Adani et al. (2011) by computing basin average root mean square (rms) of misfits (difference between observations and model simulation before data insertion) for temperature (T), salinity (S) and SLA. These are now reproduced in Figure 2 for the whole 1985-2007 reanalysis period.

The rms error decreases with depth, from a maximum at the surface, about $0.8^\circ C$ for T and $0.4 \text{ } psu$ for S, to a minimum at 1000 metres. These values are comparable with the assumed combined measurement and sampling error for each type of measurements (Adani et al. 2011). The SLA rms error is on average $4 \text{ } cm$, which is also comparable with estimates of satellite along-track altimetry error (Pujol and Larnicol 2005).

3. The time-mean general circulation

In the previous section we gave evidence that all the reanalysed state variables have a quality that is comparable to the measurement errors. This allows us to analyse the climatological structure of the general circulation inferred from the observations considered in the reanalysis for the first time. In the past, this study was attempted using geostrophic computations applied to the climatological temperature and salinity fields (Brankart and Brasseur 1998) or applying inverse methods to a much sparser data set (Tziperman and Malanotte-Rizzoli 1991). More recently, a surface current climatology was computed for the same time period considering a linear model of surface drifter trajectories and geostrophic currents from altimetry (Poulain et al. 2012), but without considering any other subsurface data.

The basic reanalysis data set used in this paper is composed of monthly mean values which were subsequently averaged in time to compose the time-mean circulation described by the mean velocity field, \vec{u}_M :

$$\vec{u}_M(\vec{x}) = \frac{1}{\tau} \int_0^\tau \vec{u}(\vec{x}, t) dt \quad (1)$$

where $\vec{u} = (u, v)$ is the horizontal velocity, τ is equal to 21 years, from 1987 to 2007, \vec{x} is the model grid positions and t is time. We allowed for a spin-up time of the analysis system of two years, 1985 and 1986, trying to minimize the effects of adjustments in the deep layers. We point out that, in view of the large decadal variability of the circulation, the 21-year average may not represent the long-term mean circulation.

a. Surface circulation

The surface mean circulation is displayed in Fig. 3 and in the following we will describe in detail the main features emerging from this climatological picture.

Starting with the Alboran Sea (Fig. 1), the circulation is characterized by the Atlantic Water current entering from Gibraltar and meandering around the two Alboran gyres. We note that the western anticyclonic Alboran gyre (Heburn and La Violette 1990) is well depicted while the eastern gyre counterpart is at a smaller amplitude. It is known that both the western and eastern gyres may disappear from time to time (Vélez-Belch et al. 2005; Snaith et al. 2003), and the eastern gyre in particular, so its amplitude in the mean is smaller than the western gyre. The Almera-Oran front (Allen et al. 2001) is a well defined mean circulation structure that lies between the eastern Alboran gyre and a cyclonic eddy that we will call here the Almera-Oran cyclonic eddy. To our knowledge this cyclonic structure has never been fully documented but it appears to be a large amplitude mean flow structure of this region.

After the Almera-Oran front two intensified currents are defined, one going northward toward the Ibiza channel (Fig. 1) and the other forming an intensified segment of the Algerian Current (Arnone et al. 1990). This is only a well-defined boundary current immediately after the Almera-Oran front, between 0° E and 2° E, whereas between 3° and 8° E the mean flow is weak and without a precise direction. This is the well-known instability region of the Algerian current (Millot 1985), where large anticyclonic eddies grow and persist for several months, dominating the flow field and moving slowly in all directions but especially eastward and coastward (Ayoub et al. 1998). The largest eastward mean velocities are found in the open ocean, in the central western Mediterranean, forming a wide meandering free jet, centred around 39.5° N. This eastward mid-ocean current has never been well documented before, and will here be called the Western Mid-Mediterranean Current (WMMC) for future reference. The WMMC is a residual current after multi-year averaging and instantaneous currents could not always show this feature.

The northward flowing segment after the Almera-Oran front feeds the WMMC, branching around the islands of Ibiza and Majorca. After Majorca, the WMMC merges with the southern border of the cyclonic flow dominating the circulation north of 40° N, called in

the literature the Gulf of Lion gyre (Madec et al. 1991; Pinardi et al. 2006). The latter is constituted by a northward boundary intensified current also called the Liguro-Provenal-Catalan Current (Pinardi et al. 2006) which closes cyclonically in the Catalan Sea.

Eastward of the Balearic Islands, the WMMC flows in the open ocean turning southward along the western coasts of Sardinia and forming there an intensified current that is the largest amplitude current in the western Mediterranean Sea, called hereafter the Southerly Sardinia Current (SSC). In the Sardinia Channel, the SSC flows along the Tunisian coastlines, forming a segment of the Algerian Current starting from 8° E. Entering the southern Tyrrhenian Sea the reformed Algerian Current branches in three parts, as documented in the past (Béranger et al. 2004; Pinardi et al. 2006). Two branches enter the Sicily Strait and a third one flows north-eastward in the Tyrrhenian Sea.

In the Tyrrhenian Sea the circulation is dominated by three cyclonic gyres: the South-Western Tyrrhenian Gyre (SWTG), the South-Eastern Tyrrhenian Gyre (SETG) and the Northern Tyrrhenian Gyre (NTG, Artale et al. (1994)). Only two of the three are well known in the literature, while the SETG is weak in the mean, most probably because this is an area of frequent anticyclonic eddies that weaken the cyclonic mean circulation (Rinaldi et al. 2010).

In the middle of the Tyrrhenian Sea, the eastern border of the SWTG forms a well-defined northward current which we call here the Middle Tyrrhenian Current (MTC). Around Corsica (see Fig. 1) there are two northward directed currents, the western and western Corsica Currents, the first being part of the Gulf of Lion Gyre border and the second being a segment of the MTC.

Thus, in conclusion, the surface western Mediterranean circulation is characterized by the well known western and eastern Alboran gyres, the Gulf of Lions gyre but also by new mean currents such as the WMMC, the SSC and the MTC. The mean Algerian Current emerges as a discontinuous structure, formed by two segments, one from 0° E to 2° E and the other from 8° E to 10° E, as originally depicted by Millot (1985). The SSC is a very

intense current in the western Mediterranean that converges with the Algerian segment to form the highest amplitude current of the Mediterranean Sea, with the sole exception of the Strait of Gibraltar. The SSC is confirmed by the recent analysis of surface drifters of Poulain et al. (2012).

The Algerian Current, entering the Sicily Strait, branches into the Sicily Strait Tunisian Current (SSTC) along the southern coasts and the Atlantic Ionian Stream (AIS) (Robinson et al. 1999; Onken et al. 2003; Lermusiaux and Robinson 2001) in the north. At about 13° E, the SSTC turns northward around a large anticyclonic gyre called by Pinardi et al. (2006) the Sirte Gyre (SG). After the Malta escarpment the AIS flows as a broad open ocean free jet located approximately around $36^{\circ} - 35.5^{\circ}$ N. The AIS forms the northern border of the SG subdividing the Ionian Sea in two meridional regions. North of the AIS, the mean flow is not very well defined, except for segments of an eastern boundary current, called for future reference the Eastern Ionian Current (EIC) and, on the western Ionian side, a weak cyclonic gyre, called the Northern Ionian Cyclonic Gyre. Another sub-basin scale coherent structure on the north-eastern side of the AIS is the Pelops Gyre (PG) (Robinson et al. 1992), which has been documented to be a recurrent large eddy.

Before entering the Cretan Passage (Fig. 1), around 20° E, the AIS turns southward reaching the North African coasts and forming a broad current from approximately 21° to 26° E which we will call hereafter the Cretan Passage Southern Current (CPSC). The latter branches in the Mid-Mediterranean Jet (MMJ) and the Southern Levantine Current (SLC) (Pinardi et al. 2006). The MMJ was first described by Golnaraghi and Robinson (1994) and is a free open ocean jet between the Mersa Matruh Gyre System (MMGS) to the south and the Rhodes Gyre to the north (Milliff and Robinson 1992). The MMJ widens around 31° E branching into a southern and a western Cyprus current, both of which join the Asia Minor Current (Robinson et al. 1991; Özsoy et al. 1993). The latter forms the northern intensified boundary current of the RG. South of the MMJ branches, what is known as the Shikmona Gyre System (Hecht et al. 1988; Pinardi et al. 2006; Zodiatis et al. 2005) dominates the

mean flow.

In the northern part of the Cretan Passage, directly before the Strait of Kassos (Fig. 1), the continuation of the Asia Minor Current forms a large anticyclonic meander, immediately after the Rhodes Gyre, encircling the area of the recurrent anticyclonic Ierapetra Gyre (Robinson et al. 1991). This structure has mainly been documented by different satellite altimetry analysis studies (Pujol and Larnicol 2005; Isern-Fontanet et al. 2003).

The two Mediterranean marginal seas, the Aegean and Adriatic, generally show a cyclonic circulation. The Adriatic Sea is dominated by the Middle and Southern Adriatic cyclonic gyres and the Eastern Adriatic Current and the Western Adriatic Coastal Current systems (Artegiani et al. 1997). The Aegean Sea shows a southward flow through the Cyclades (Fig. 1), called for future reference the Southward Cyclades Current (SCC) and a wide westward current in the middle of the Sea of Crete, which we call the Cretan Sea Westward Current (CSWC). North of the Dardanelles outflow the time-mean circulation is dominated by a well-defined and high-intensity anticyclonic gyre (Kourafalou and Barbopoulos 2003), called the North Aegean Sea Antyclone (NASA). On the eastern side of the Cyclades (Fig. 1) the Eastern Cyclades Southward Current is a well-defined mean circulation structure.

In the Eastern Mediterranean the circulation is very close to what was depicted by the early basin-scale circulation studies (Robinson et al. 1992) and (Malanotte-Rizzoli and the Liwex Group 2003). The new feature captured by the multi-decadal mean is the subdivision of the Ionian Sea into northern and southern regions by the free flowing jet of the AIS. In the last section of the paper we will overview the new and consolidated structures of the general circulation.

b. Intermediate depth circulation

The intermediate depth circulation structure is shown in Fig. 4 as the average currents between 200 and 300 metres depth. This layer can be taken as representative of the LIW layer in the Eastern Mediterranean. The circulation at this depth has never been mapped

adequately from observational data sets since the level of no-motion assumption involved in past calculations (Brankart and Brasseur 1998; Tziperman and Malanotte-Rizzoli 1991) considerably affects the circulation estimates.

The LIW layer circulation is a component of the subsurface recirculation flow exiting at Gibraltar (Pinardi and Masetti 2000), and thus generally flows in the opposite direction to the surface flow at the Strait of Sicily and in the Algerian and Alboran Seas. We will start our description this time from the Levantine Sea, which is the area of formation of LIW. The basin-scale cyclonic area of the Rhodes Gyre and the Cretan Passage is consistent with the surface flow and the Ierapetra Gyre meander signature is also evident at depth. The Mersa Matruh Gyre shows at depth a multipolar structure due to a large meander of the MMJ and a large-amplitude anticyclone with respect to the surface circulation, near the Egyptian coasts. The Shikmona Gyre System is defined at depth by several anticyclonic semi-stationary eddies, up to the Syrian offshore areas (Hecht et al. 1988; Brenner et al. 1991).

In the Cretan Passage differences emerge with respect to the surface flow field (Fig. 3): the cyclonic turn of the currents westward of Crete (Fig. 1) now clearly defines the Western Cretan Cyclonic Gyre (WCCG). In the Sea of Crete, the surface Cretan Sea Westward Current (CSWC) also has a well-defined structure at this depth, exiting the Kithira Strait (Fig. 1) and branching in the Ionian Sea into three streams. The first forms the southern border of the Pelops Gyre, the second turns eastward while the other shoots southward joining the Sirte Gyre anticyclonic flow. The reanalysis intermediate depth mean flow indicates that the preferred path for the LIW is southward, along the Gulf of Sirte shelf break as part of the large scale transport of the anticyclonic SG. The well-known westward LIW current of the Sicily Strait (Sparnocchia et al. 1999; Pinardi et al. 2006) emerges as a branching of the SG south-western intensified current.

Northward of the surface AIS position the mean flow is weak, but at this depth it is now evident that a cyclonic motion or gyre prevails. This cyclonic gyre, called the Northern

Ionian Cyclonic Gyre (NICG), is separated from the AIS by a region of weak flow generated by averaging the AIS excursions and meandering instabilities.

Entering the Western Mediterranean, the LIW current turns cyclonically around the SWTG, breaking into current segments that bring LIW across the Corsica Strait and into the Algerian basin through the Sardinia Channel. The LIW path is characterized by two major branches starting approximately at 6° E one directed northward, toward the Gulf of Lion Gyre and the second westward toward the Strait of Gibraltar. At this depth the Gulf of Lion Gyre is multi-centric, with its southern border shifted to the south and several cyclonic circulation structures inside the larger-scale gyre.

The emerging picture of the Mediterranean Sea mean circulation at intermediate depth shows a basin dominated by intense jets, gyres and large scale eddies, as at the surface. While cyclonic motion is mainly organized in large scale gyres, anticyclonic motion is at the scale of the large eddies with the exception of the Sirte Gyre. The mean path of the LIW emerges after the Cretan Passage from the Sirte Gyre south-western intensified border currents, while in the western Mediterranean it has at least two main directions, one toward the Gulf of Lion Gyre and the second directly across the Algerian basin, toward the Strait of Gibraltar. The latter is the residual of a complex eddy flow field that itself moves westward in the offshore areas of the Algerian basin and advects filaments of LIW at its borders (Puillat et al. 2006).

4. Decadal variability of general circulation

The second most important finding of studies of the past two decades is that the Mediterranean Sea circulation variability peaks at the seasonal and interannual time scales, as is documented by observations (Larnicol et al. 2002; Manca et al. 2006; Gacic et al. 2011; Poulain et al. 2012) and model simulations (Pinardi et al. 1997; Korres et al. 2000; Molcard et al. 2002; Demirov and Pinardi 2002). In this section we will concentrate attention on

the decadal changes occurring between the first (1987-1996, hereafter called Period A) and the second (1997-2006, hereafter called Period B) decades. Period A was chosen because it coincides with a stable positive North Atlantic Oscillation-NAO index (Hurrell 2003) and it overlaps with the EMT event period (Gertman et al. 2006) while Period B was simply the remaining part of the available reanalysis time series.

In Figure 5 we show the surface circulation averaged in the two periods. In the western Mediterranean Sea, the largest surface changes between the two periods occur in the Alboran and Tyrrhenian Seas. In the Alboran Sea, the western anticyclonic gyre is weak while the Almera-Oran front is strong in Period A, while during Period B the western anticyclonic gyre is strong and the Almera-Oran front is weak and the first segment of the Algerian Current hugs the coasts up to $3 - 4^{\circ}$ E. The Tyrrhenian circulation shows larger-amplitude cyclonic gyres, the SWTG, SETG and NTG during Period B, while in Period A all of them are noticeably weaker.

The largest changes between Period A and B occur in the Eastern Mediterranean Sea where a current reversal takes place in the northern Ionian Sea and large differences in gyre location and current amplitudes are visible in the Cretan Passage and the Levantine basin. In the Ionian Sea the AIS shows a large northward meander in Period A giving rise to an overall anticyclonic circulation in the northern part of the basin. The picture of the circulation emerging in Period A is congruent with the previous estimates from single cruises (Robinson et al. 1999; Malanotte-Rizzoli et al. 1997). On the other hand, during Period B the circulation in the northern Ionian is cyclonic and the AIS cuts across the basin, remaining at the latitude of 36° N after the Maltese escarpment. We call these decadal changes the Northern Ionian Reversal phenomenon that is connected at the surface with shifts of the AIS position.

During Period B the Levantine Sea cyclonic surface circulation strengthened and structures like the Asia Minor Current and the Pelops Gyre grew in amplitude compared to Period A. In Period B the Mersa Matruh Gyre seems to be more convoluted, forming a dipole with

the cyclonic meander of the MMJ. The Ierapetra Gyre meander is deeper and better formed in Period B than in Period A.

In the 200-300 m layer, Fig. 6, the decadal changes are again largest in the Eastern Mediterranean. The surface Northern Ionian Reversal phenomenon is evident at intermediate depth: during Period B the northern Ionian cyclonic gyre is western-boundary intensified and the LIW subsurface flow, through the Sicily Strait, is at larger amplitudes than in Period A. In the Levantine basin the intermediate depth circulation between Period A and B is qualitatively similar with the exception of the number of large anticyclonic and cyclonic eddies.

In the Western Mediterranean the largest change is represented by the southward extension of the Gulf of Lion Gyre, which is formed by two cyclonic centers during Period B, extending one degree further to the south than in Period A. The mean path of the LIW is always along the Algerian coasts, but during Period B a southward branch of the Gulf of Lion gyres reinforces the westward flow toward the Strait of Gibraltar.

It is evident from the basin scale analysis that the Northern Ionian Reversal phenomenon is the largest decadal variability event of the Mediterranean Sea in the past 20 years. The phenomenon is associated with the shift of the AIS northward in Period A and the emergence of a cyclonic circulation, north of the central position of the AIS, in Period B. Poulain et al. (2012) also describes this reversal for almost exactly the same two periods from surface drifters and satellite altimetry and this change was already documented by (Borzelli et al. 2009). All these studies agree in setting the time of the surface reversal to 1997: in our analysis Period A starts in 1987, but longer reanalysis reconstructions are needed to check the real periodicity, if any, of the Northern Ionian Reversal phenomenon.

Several large-scale modelling studies have documented a reversal from cyclonic to anticyclonic around 1987, from the beginning of the eighties onwards (Korres et al. 2000; Demirov and Pinardi 2002) . In fact, these previous authors connected the first Northern Ionian Reversal in 1987 with changes in the prevalent wind stress curl sign over the basin. Demirov

and Pinardi (2002) analyse a simulation where the circulation in the northern Ionian was cyclonic between 1980 and 1987, similar to that now found in Period B, then reversing to anticyclonic in 1987.

5. Barotropic wind-driven circulation

In this section we want to show the barotropic structure of the circulation as depicted by the vertically-integrated flow field, i.e. $\vec{u} = \frac{1}{H} \int_{-H}^0 \vec{u} dz$ where H is the bottom depth. The barotropic streamfunction will be then computed as:

$$\vec{u} = \hat{k} \times \nabla \psi \quad (2)$$

where $\hat{k} = (0, 0, 1)$. The analysis of the barotropic flow field will highlight the structure of the wind driven circulation that is an important component of the surface and intermediate depth circulation previously described.

In Fig. 7 the long-term and decadal mean barotropic streamfunction is shown. As expected, the streamfunction is characterized by sub-basin-scale gyres and eddy-like structures. Northern, open ocean regions are characterized in the multi-decadal mean by cyclonic gyres both in the western and eastern Mediterranean: the exceptions are the Ionian Sea and the Tyrrhenian Sea. The latter is characterized by an overall multi-centric cyclonic gyre, as described in the mean surface circulation of Fig. 3. The northern Ionian Sea is characterized, on the other hand, by large-scale gyre-like structures of opposite sign for the 21-year mean streamfunction while the two decadal mean fields change sign due to the Northern Ionian Reversal phenomenon.

In the multi-decadal mean the southern regions are generally characterized by anticyclonic, eddy-like structures except for the southern Ionian basin where the large scale Sirte Gyre (SG) dominates. In general, the western Mediterranean and Levantine Sea southern regions are dominated by anticyclonic semi-permanent large-scale eddies that, as discussed

in the introduction, could be indicative of baroclinic instability and geostrophic turbulence inverse cascade mechanisms.

The Algerian basin, the northern Ionian Sea and the southern Levantine basin are undergoing the largest changes in streamfunction between Periods A (1987-1996) and B (1997-2006). In particular, it is evident that in Period B the western Mediterranean is characterized by a southward extension of the Gulf of Lion Gyre, joining the cyclonic motion along the Algerian Current. The same seems to happen in Period B in the Levantine Sea, where the Rhodes Gyre cyclonic circulation extends further to the south, confining the barotropic anticyclonic motion closer to the North African coasts compared to Period A.

The analysis of the barotropic flow field shows that the wind driven circulation subdivides the basin into northern cyclonic and southern anticyclonic gyres as previously depicted by Pinardi and Navarra (1993) and Pinardi and Masetti (2000) from low resolution simulations. There is an evident correlation between the barotropic flow field of Fig. 7 and the surface and intermediate depth circulation (Fig. 3, 4) structures, showing the importance of the barotropic component of the basin scale mean circulation.

The barotropic wind driven circulation was also studied for Period A by Molcard et al. (2002) and it was shown that correlation between wind stress curl and the flow field in the Mediterranean Sea is as high as in the mid-latitude North Atlantic regions. Fig. 8 displays the average wind stress and the wind stress curl: the northern, cyclonic (southern, anticyclonic) regions are associated with positive (negative) wind stress curl. In the northern Ionian, the average wind stress curl changes sign between the Period A and B decades. Such changes are correlated with the streamfunction changes between the two periods, thus supporting the interpretation that the wind stress curl could play an important role in the Northern Ionian Reversal phenomenon which has not been pointed out by previous analyses such as Borzelli et al. (2009) and Gacic et al. (2011).

6. Water Mass Formation variability

One of the most important processes occurring in the Mediterranean Sea is the formation of intermediate and deep water masses and the reanalysis offers the opportunity to revisit the Water Mass Formation (WMF) rate variability and events for the past 20 years.

Here we will concentrate on the intermediate and deep water formation rates occurring in the 4 regions reproduced in Fig. 1. Region 1 contains the central part of the Rhodes Gyre and is a well-known region for Levantine Intermediate Water formation (LIW), while region 2 is in the Sea of Crete and is the site of formation of what is known as Cretan Deep Water (CDW). Region 3 is the area where open ocean deep convection occurs and Eastern Mediterranean Deep Waters (EMDW) are formed. Finally, Region 4 is the Western Mediterranean Deep Water (WMDW) formation area.

Tziperman and Speer (1994) have computed the water mass formation rate from surface buoyancy fluxes which give an upper limit for the water that could be transformed from light surface to heavy intermediate and deep waters. Our estimate of WMF rate is done following the method of Lascaratos et al. (1993), which consists of estimating for each year the volume of waters on a specified density interval in the mixed layer of a specific area of interest, and then dividing this volume by one year in seconds. This choice is due to the fact that we believe our estimate of the surface mixed layer properties is more accurate than the estimates of the surface fluxes due to data assimilation of temperature and salinity profiles in the surface layers. The thresholds for the mixed layer densities, corresponding to the different water masses, are reported in Table 1 for each area, taken from Castellari et al. (2000).

The upper panel of Fig. 9 shows the winter monthly rates averaged over the period 1987-2007 in the different areas, using the mixed layer density lower thresholds described in Table 1. The largest rates are always reached during February and March, in every area, with a tendency of the Gulf of Lion to produce more deep waters in February than March. Summing the winter rate values, the WMF rates over the 1987-2007 period amount to 0.7

Sv for LIW, 0.3 and 0.4 Sv for EMDW and CDW respectively and 0.9 Sv for WMDW. These numbers compare well with all the past estimates and show that the LIW and WMDW rates are more than double the EMDW and CDW rates.

If we now calculate the WMF rates for each year, we obtain the lower panel of Fig. 9 where four large event periods appear in the time series. The first large WMF event in Fig. 9 occurs in the Gulf of Lion area in 1987 as documented by Leaman (1991). It is an open ocean formation event which produced a large amount of WMDW, larger than found previously in the MEDOC experiment (GROUP 1970).

The second event period is the LIW and Levantine Deep Water (LDW) formation process documented by Gertman et al. (1994) and the Eastern Mediterranean Transient (EMT) CDW large formation event (Roether et al. 1996) occurring between 1992-1993. It is clear from the reanalysis that CDW reached maximum rates in 1992-1993 (larger than 1 Sv) together with LIW and EMDW and that the 1987-1991 period showed consistent formation of both CDW and LIW. Moreover, during the years 1990-1993 the LIW formed was in large part LDW, since, using the higher density threshold of Table 9, we obtain values that are about 80% of the lower threshold rates.

This remarkable CDW formation event ends abruptly after 1996 and is not reproduced in the ten years following. Many theories have been put forward to explain the start and origin of the EMT, based upon model simulations and other experimental evidence, from the first modelling paper of Wu et al. (2000) to the more recent observations of Gertman et al. (2006) and the latest modelling efforts of Beuvier et al. (2010). We argue that the EMT reproduced in the reanalysis is the result of several concomitant factors: the Northern Ionian Reversal phenomenon which diverted Atlantic waters from entering the Levantine Sea, as already discussed by Malanotte-Rizzoli et al. (1999), increasing the salinity in that area, the entrance of saltier LIW/LDW from the Rhodes basin straits, the lower flux of fresh Black Sea waters in the northern Aegean and the large air-sea flux losses in the winters of 1992 and 1993. The reanalysis contains all these concomitant factors, except for the omission of

the changes in Black Sea water outflow, and was able to reproduce the formation of CDW at the right time.

The third event in Fig. 9 occurs in 1999 and 2000 in the Gulf of Lion and the Adriatic Sea. The 1999 event in the Adriatic Sea is documented by Manca et al. (2006) and has been connected to saltier waters entering at mid-depth from Otranto, a consequence of the CDW spreading connected to the EMT, and to the intensity of the buoyancy losses in 1999-2000.

The fourth event in Fig. 9 occurs in 2005 and 2006 in the Gulf of Lion, as well as in the Adriatic Sea and the Rhodes Gyre area. The WMDW large rates are documented by a recent paper (Smith et al. 2008) and the reanalysis captures the process, concomitant to another equivalent WMF event occurring in the Ligurian Sea (not shown). The explanation for this large event and its unusually large formation area is given by (Herrmann et al. 2010) in terms of increase in salinity of the western Mediterranean waters and large heat losses: for the increase in salinity we describe the process in the next section.

If the largest density thresholds of Table 1 were used, the qualitative behavior of the time series in Fig. 9 would not change except for area 3 where the amount would change by 50% probably due to the large uncertainties in the heat and water fluxes, missing processes in the model and the scarcity of assimilated data.

In order to see when the EMT waters arrived in the western Mediterranean, we have calculated the salinity below 200 m across the westernmost section of the Sicily Strait (see Fig. 10). It is clear then that in 2000-2001 waters 0.12 PSU saltier than in the previous period started to arrive in the western Mediterranean, supporting the idea that part of the salt increase in the intermediate waters in the western Mediterranean is connected to the EMT. However, as we will see later, the process of salinization of the western Mediterranean started earlier than the year 2000.

In synthesis, study of WMF rates for the past 20 years confirms some general concepts already present in the literature: large deep and intermediate water formation events in the Rhodes, southern Adriatic and Gulf of Lion areas occur with a frequency of three to six

years. For the deep water of the Sea of Crete, the CDW, we show that CDW already started to be formed from 1987 onwards, and after 1996 decayed permanently. The Rhodes Gyre area is confirmed as being an area of frequent deep water formation events and 2005-2006 is the largest deep water formation event of the past 23 years in the Mediterranean Sea.

a. Deep water mass characteristic changes

A view of the changes occurring in the water mass characteristics, associated with the WMF events just described, is given by Fig. 11. In the upper panel we show the February-March yearly average θ/S diagram for the southern Adriatic region. The water mass properties change abruptly from 1999 with respect to the previous 12-year period (1987-1998). The shift is associated with larger salinity and warmer temperature intermediate waters entering from the Otranto Strait. This is connected to the spreading of the EMT event that reached the Otranto Strait increasing the salinity of the entering intermediate waters in the southern Adriatic Sea.

The February-March average θ/S diagram for the Gulf of Lion (region 4) shows step-like changes in θ/S characteristics for the past 23 years, all of them in the direction of increasing the salinity and the temperature of the deep water masses, as documented very early by Rohling and Bryden (1992). In this picture, however, we show that between 1987 and 1988 we have the largest single increase in salt and temperature, followed by 1993 and 1999. The 1988 and 1993 steps are not connected to special WMDW events in the Western Mediterranean (Fig. 9), and thus are supposedly a deep water mass redistribution process. The increase of 0.1 PSU and $0.2^{\circ}C$ in the θ/S characteristics of the deep waters in the Gulf of Lion between 1987 and 1999 is presumably determined within the western Mediterranean Sea by a combination of Gibraltar inflow, spreading mechanisms and surface buoyancy fluxes.

7. Conclusions

In this paper we have described the mean circulation of the Mediterranean Sea emerging from a 23-year eddy-permitting reanalysis. The multi-decadal mean flow emerging from this analysis is consistent with many of the previous findings but new circulation structures also become apparent.

A schematic of the surface and intermediate general circulation emerging from this analysis is presented in Fig. 12, where we have named currents and gyres for future reference (see Table 2). The most important difference with respect to previous schematics and studies is the appearance of more defined open ocean, free jet intensified structures: the first, is the Western Mid-Mediterranean Current, the second the Atlantic-Ionian Stream and the third the Mid-Mediterranean Jet (MMJ). Furthermore, it is found that the largest amplitude currents are found at the Gibraltar Atlantic Water entrance, in boundary intensified currents around the Gulf of Lion Gyre and the Rhodes Gyre, in the Sardinia and Cretan Passages. The presence of a persistent, recurrent eddy-field which is not averaged out by the multi-decadal mean is shown in the Algerian basin, between 3° and 8° E, in the Aegean arc areas and in the southeastern Levantine Sea.

The barotropic stream function field confirms that the surface circulation is strongly connected to the barotropic flow field. The large-scale wind-driven barotropic gyres reinforce the picture of a northern basin dominated by cyclonic gyres and a southern one characterized by anticyclonic gyres and eddies.

The single most important decadal variability event in the basin occurs in the northern Ionian Sea, where a current reversal phenomenon is documented to occur after 1997. Prior to this date, the Atlantic Ionian Stream (AIS) was occupying the northern Ionian Sea, producing an overall anticyclonic circulation structure, while after 1997 the AIS remains in the middle of the Ionian basin and a cyclonic gyre develops at its northern limits. This is the first time that a clear picture of the Northern Ionian Reversal phenomenon has emerged, due to the high space-time consistency of the reanalysis fields. The Ionian reversal mechanism is

also evident in the streamfunction, thus giving further evidence of the wind-driven nature of the mechanisms underlying the northern Ionian reversal.

At middle depth, between 200 and 300 m, the circulation is similar to the surface except for the LIW return flow at the Sicily Strait. We have documented for the first time the fact that the mean path of the LIW toward the Sicily Strait may be along the Lybian coasts as part of an intensified current at the border of the Sirte Gyre.

The WMF study documents that four major events occurred in the basin. Both intermediate and deep water is formed at the same time in certain years, and the largest WMF event of the past 23 years occurred in the Western Mediterranean in 2005-2006. The CDW formation event and the EMT process is well captured by the model, and it is found that CDW starts to be formed in 1987 and then stops after 1996. In 1999, the EMT higher salinity LIW entered the Adriatic Sea, and in 2000-2001 the EMT modified LIW crossed the Sicily Strait, presumably conditioning the large WMDW event of 2005-2006.

The changes in winter water mass characteristics of the past 23 years in the EMDW and WMDW regions occur at different time scales: the winter deep EMDW T/S characteristics change due to the 1999 arrival of the saltier LIW and CDW waters during the spreading phase of the EMT, while the WMDW changes start in 1988 and occur through four steps. The total salinity change in twenty years for the EMDW is 0.1 PSU and is 0.14 PSU for the WMDW, while potential temperature changes are 0.2 °C for both.

It is clear that the reanalysis is a valuable tool for studying ocean dynamics in limited areas of the ocean, provided the model and the data assimilation are high resolution. However, future work should consider a thorough analysis of the uncertainties associated with the derived reanalysis fields in order to further benefit from the continuous and homogeneous reanalysis time series.

Acknowledgments.

This work is dedicated to the outstanding contribution of Prof. A.R.Robinson to our understanding of Mediterranean Sea circulation. The scrupulous and innovative observational and modelling strategy he implemented in the decadal program of the Physical Oceanography of the Eastern Mediterranean was the beginning of a new era of research in this basin and laid the foundations for successful implementation of an operational oceanographic system for the Mediterranean Sea. The work of this paper was financed: by the EU CIRCE project, the University of Bologna Ph.D. programme in Geophysics for Dr. M.Adani, for the CMCC authors by the Italian Ministry of Education, University and Research and the Italian Ministry of Environment, Land and Sea under the GEMINA project, for INGV authors by the NEXTDATA Project.

REFERENCES

- Adani, M., S. Dobricic, and N. Pinardi, 2011: Quality assessment of a 1985–2007 mediterranean sea reanalysis. *Journal of Atmospheric and Oceanic Technology*, **28** (4), 569–589, doi:10.1175/2010JTECHO798.1, URL <http://dx.doi.org/10.1175/2010JTECHO798.1>.
- Allen, J. T., D. A. Smeed, J. Tintoré, and S. Ruiz, 2001: Mesoscale subduction at the almeria-oran front: Part 1: Ageostrophic flow. *Journal of Marine Systems*, **30** (3-4), 263–285, URL <http://www.sciencedirect.com/science/article/pii/S0924796301000628>.
- Arnone, R. A., D. A. Wiesenburg, and K. D. Saunders, 1990: The origin and characteristics of the algerian current. *J. Geophys. Res.*, **95** (C2), 1587–1598, doi:10.1029/JC095iC02p01587, URL <http://dx.doi.org/10.1029/JC095iC02p01587>.

- Artale, V., M. Astraldi, G. Buffoni, and G. P. Gasparini, 1994: Seasonal variability of gyre-scale circulation in the northern tyrrhenian sea. *J. Geophys. Res.*, **99** (C7), 14 127–14 137, doi:10.1029/94JC00284, URL <http://dx.doi.org/10.1029/94JC00284>.
- Artegiani, A., E. Paschini, A. Russo, D. Bregant, F. Raicich, and N. Pinardi, 1997: The adriatic sea general circulation. part ii: Baroclinic circulation structure. *Journal of Physical Oceanography*, **27** (8), 1515–1532, doi:10.1175/1520-0485(1997)027<1515:TASGCP>2.0.CO;2, URL [http://dx.doi.org/10.1175/1520-0485\(1997\)027<1515:TASGCP>2.0.CO;2](http://dx.doi.org/10.1175/1520-0485(1997)027<1515:TASGCP>2.0.CO;2).
- Ayoub, N., P.-Y. Le Traon, and P. De Mey, 1998: A description of the mediterranean surface variable circulation from combined ers-1 and topex/poseidon altimetric data. *Journal of Marine Systems*, **18** (1-3), 3–40, URL <http://www.sciencedirect.com/science/article/pii/S0924796398800043>.
- Béranger, K., L. Mortier, G. P. Gasparini, L. Gervasio, M. Astraldi, and M. Crépon, 2004: The dynamics of the sicily strait: a comprehensive study from observations and models. *Deep Sea Research Part II: Topical Studies in Oceanography*, **51** (4-5), 411–440, URL <http://www.sciencedirect.com/science/article/pii/S096706450400027X>.
- Beuvier, J., et al., 2010: Modeling the mediterranean sea interannual variability during 1961-2000: Focus on the eastern mediterranean transient. *J. Geophys. Res.*, **115** (C8), doi:10.1029/2009JC005950, URL <http://dx.doi.org/10.1029/2009JC005950>.
- Borzelli, G. L. E., M. Gacic, V. Cardin, and G. Civitarese, 2009: Eastern mediterranean transient and reversal of the ionian sea circulation. *Geophys. Res. Lett.*, **36** (15), L15 108, doi:10.1029/2009GL039261, URL <http://dx.doi.org/10.1029/2009GL039261>.
- Brankart, J. M. and P. Brasseur, 1998: The general circulation in the mediterranean sea: a climatological approach. *Journal of Marine Systems*, **18** (1-3), 41–70, URL <http://www.sciencedirect.com/science/article/pii/S0924796398000050>.

- Brenner, S., Z. Rozentraub, J. Bishop, and M. Krom, 1991: The mixed-layer/thermocline cycle of a persistent warm core eddy in the eastern mediterranean. *Dynamics of Atmospheres and Oceans*, **15** (3–5), 457–476, URL <http://www.sciencedirect.com/science/article/pii/037702659190028E>.
- Buongiorno Nardelli, B., G. Larnicol, E. D’Acunzo, R. Santoleri, S. Marullo, and P. Y. Le Traon, 2003: Near real time sla and sst products during 2-years of mfs pilot project: processing, analysis of the variability and of the coupled patterns. *Annales Geophysicae*, **21** (1), 103–121, doi:10.5194/angeo-21-103-2003, URL <http://www.ann-geophys.net/21/103/2003/>.
- Castellari, S., N. Pinardi, and K. Leaman, 1998: A model study of air–sea interactions in the mediterranean sea. *Journal of Marine Systems*, **18** (1–3), 89–114, URL <http://www.sciencedirect.com/science/article/pii/S0924796398900070>.
- Castellari, S., N. Pinardi, and K. Leaman, 2000: Simulation of water mass formation processes in the mediterranean sea: Influence of the time frequency of the atmospheric forcing. *J. Geophys. Res.*, **105** (C10), 24 157–24 181, doi:10.1029/2000JC900055, URL <http://dx.doi.org/10.1029/2000JC900055>.
- Demirov, E. and N. Pinardi, 2002: Simulation of the mediterranean sea circulation from 1979 to 1993: Part i. the interannual variability. *Journal of Marine Systems*, **33–34** (0), 23–50, URL <http://www.sciencedirect.com/science/article/pii/S0924796302000519>.
- Dobricic, S. and N. Pinardi, 2008: An oceanographic three-dimensional variational data assimilation scheme. *Ocean Modelling*, **22** (3–4), 89–105, URL <http://www.sciencedirect.com/science/article/pii/S1463500308000176>.
- Dobricic, S., N. Pinardi, M. Adani, M. Tonani, C. Fratianni, A. Bonazzi, and V. Fernandez, 2007: Daily oceanographic analyses by mediterranean forecasting system at the basin scale.

- Ocean Science*, **3** (1), 149–157, doi:10.5194/os-3-149-2007, URL <http://www.ocean-sci.net/3/149/2007/>.
- Gacic, M., et al., 2011: On the relationship between the decadal oscillations of the northern ionian sea and the salinity distributions in the eastern mediterranean. *J. Geophys. Res.*, **116** (C12), doi:10.1029/2011JC007280, URL <http://dx.doi.org/10.1029/2011JC007280>.
- Garrett, C., R. Outerbridge, and K. Thompson, 1993: Interannual variability in mediterranean heat and buoyancy fluxes. *Journal of Climate*, **6** (5), 900–910, doi:10.1175/1520-0442(1993)006<0900:IVIMHA>2.0.CO;2, URL [http://dx.doi.org/10.1175/1520-0442\(1993\)006<0900:IVIMHA>2.0.CO;2](http://dx.doi.org/10.1175/1520-0442(1993)006<0900:IVIMHA>2.0.CO;2).
- Gertman, I., I. Ovchinnikov, and Y. Popov, 1994: Deep convection in the eastern basin of the mediterranean sea. *Oceanology*, **34**, 19–25.
- Gertman, I., N. Pinardi, Y. Popov, and A. Hecht, 2006: Aegean sea water masses during the early stages of the eastern mediterranean climatic transient (1988–90). *Journal of Physical Oceanography*, **36** (9), 1841–1859, doi:10.1175/JPO2940.1, URL <http://dx.doi.org/10.1175/JPO2940.1>.
- Golnaraghi, M. and A. R. Robinson, 1994: Dynamical studies of the eastern mediterranean circulation. *Ocean processes in climate dynamics: Ocean processes in climate dynamics: global and mediterranean examples*, P. Malanotte-Rizzoli and A. R. Robinson, Eds., Kluwer Academic Publishers, NATO Science Series C, Vol. 419, 437.
- GROUP, M., 1970: Observation of formation of deep water in the mediterranean sea, 1969. *Nature*, **227** (5262), 1037–1040, URL <http://dx.doi.org/10.1038/2271037a0>.
- Heburn, G. W. and P. E. La Violette, 1990: Variations in the structure of the anticyclonic gyres found in the alboran sea. *J. Geophys. Res.*, **95** (C2), 1599–1613, doi:10.1029/JC095iC02p01599, URL <http://dx.doi.org/10.1029/JC095iC02p01599>.

- Hecht, A., N. Pinardi, and A. R. Robinson, 1988: Currents, water masses, eddies and jets in the mediterranean levantine basin. *Journal of Physical Oceanography*, **18** (10), 1320–1353, doi:10.1175/1520-0485(1988)018<1320:CWMEAJ>2.0.CO;2, URL [http://dx.doi.org/10.1175/1520-0485\(1988\)018<1320:CWMEAJ>2.0.CO;2](http://dx.doi.org/10.1175/1520-0485(1988)018<1320:CWMEAJ>2.0.CO;2).
- Herrmann, M., F. Sevault, J. Beuvier, and S. Somot, 2010: What induced the exceptional 2005 convection event in the northwestern mediterranean basin? answers from a modeling study. *J. Geophys. Res.*, **115** (C12), C12 051, doi:10.1029/2010JC006162, URL <http://dx.doi.org/10.1029/2010JC006162>.
- Hurrell, J. W., 2003: *CLIMATE VARIABILITY | North Atlantic and Arctic Oscillation*, 439–445. Academic Press, Oxford, URL <http://www.sciencedirect.com/science/article/pii/B0122270908001093>.
- Isern-Fontanet, J., E. García-Ladona, and J. Font, 2003: Identification of marine eddies from altimetric maps. *Journal of Atmospheric and Oceanic Technology*, **20** (5), 772–778, doi:10.1175/1520-0426(2003)20<772:IOMEFA>2.0.CO;2, URL [http://dx.doi.org/10.1175/1520-0426\(2003\)20<772:IOMEFA>2.0.CO;2](http://dx.doi.org/10.1175/1520-0426(2003)20<772:IOMEFA>2.0.CO;2).
- Korres, G., N. Pinardi, and A. Lascaratos, 2000: The ocean response to low-frequency interannual atmospheric variability in the mediterranean sea. part i: Sensitivity experiments and energy analysis. *Journal of Climate*, **13** (4), 705–731, doi:10.1175/1520-0442(2000)013<0705:TORTLF>2.0.CO;2, URL [http://dx.doi.org/10.1175/1520-0442\(2000\)013<0705:TORTLF>2.0.CO;2](http://dx.doi.org/10.1175/1520-0442(2000)013<0705:TORTLF>2.0.CO;2).
- Kourafalou, V. H. and K. Barbopoulos, 2003: High resolution simulations on the north aegean sea seasonal circulation. *Annales Geophysicae*, **21** (1), 251–265, doi:10.5194/angeo-21-251-2003, URL <http://www.ann-geophys.net/21/251/2003/>.
- Larnicol, G., N. Ayoub, and P. Y. Le Traon, 2002: Major changes in mediterranean sea level variability from 7 years of topex/poseidon and ers-1/2 data. *Journal of Marine Sys-*

tems, **33–34 (0)**, 63–89, URL <http://www.sciencedirect.com/science/article/pii/S0924796302000532>.

Lascaratos, A., R. G. Williams, and E. Tragou, 1993: A mixed-layer study of the formation of levantine intermediate water. *J. Geophys. Res.*, **98 (C8)**, 14 739–14 749, doi:10.1029/93JC00912, URL <http://dx.doi.org/10.1029/93JC00912>.

Leaman, F. A. S., Kevin D., 1991: Hydrographic structure of the convection regime in the gulf of lions: Winter 1987. *J. Phys. Oceanogr.*, **21**, 575–598.

Lermusiaux, P. and A. Robinson, 2001: Features of dominant mesoscale variability, circulation patterns and dynamics in the strait of sicily. *Deep Sea Research Part I: Oceanographic Research Papers*, **48 (9)**, 1953 – 1997, doi:10.1016/S0967-0637(00)00114-X, URL <http://www.sciencedirect.com/science/article/pii/S096706370000114X>.

Ludwig, W., E. Dumont, M. Meybeck, and S. Heussner, 2009: River discharges of water and nutrients to the mediterranean and black sea: Major drivers for ecosystem changes during past and future decades? *Progress In Oceanography*, **80 (3-4)**, 199–217, URL <http://www.sciencedirect.com/science/article/pii/S0079661109000020>.

Madec, G., P. Delecluse, M. Crepon, and M. Chartier, 1991: A three-dimensional numerical study of deep-water formation in the northwestern mediterranean sea. *Journal of Physical Oceanography*, **21 (9)**, 1349–1371, doi:10.1175/1520-0485(1991)021<1349:ATDNSO>2.0.CO;2, URL [http://dx.doi.org/10.1175/1520-0485\(1991\)021<1349:ATDNSO>2.0.CO;2](http://dx.doi.org/10.1175/1520-0485(1991)021<1349:ATDNSO>2.0.CO;2).

Maillard, C., et al., 2005: A mediterranean and black sea oceanographic database and network. *Bollettino di Geofisica Teorica ed Applicata*, **46 (4)**, 329–343.

Malanotte-Rizzoli, P., B. B. Manca, M. R. d’Alcala, A. Theocharis, S. Brenner, G. Budillon, and E. Ozsoy, 1999: The eastern mediterranean in the 80s and in the 90s: the

- big transition in the intermediate and deep circulations. *Dynamics of Atmospheres and Oceans*, **29** (2–4), 365–395, URL <http://www.sciencedirect.com/science/article/pii/S0377026599000111>.
- Malanotte-Rizzoli, P. and the Liwex Group, 2003: The levantine intermediate water experiment (liwex) group: A laboratory for multiple water mass formation processes. *J. Geophys. Res.*, **108** (C9), doi:10.1029/2002JC001643, URL <http://dx.doi.org/10.1029/2002JC001643>.
- Malanotte-Rizzoli, P., et al., 1997: A synthesis of the ionian sea hydrography, circulation and water mass pathways during poem-phase i. *Progress In Oceanography*, **39** (3), 153–204.
- Manca, B. B., V. Ibello, M. Pacciaroni, P. Scarazzato, and A. Giorgetti, 2006: Ventilation of deep waters in the adriatic and ionian seas following changes in thermohaline circulation of the eastern mediterranean. *Climate Research*, **31** (2-3), 239–256, URL <http://www.int-res.com/abstracts/cr/v31/n2-3/p239-256/>.
- Manzella, G. M. R., et al., 2007: The improvements of the ships of opportunity program in mfs-tep. *Ocean Science*, **3** (2), 245–258, doi:10.5194/os-3-245-2007, URL <http://www.ocean-sci.net/3/245/2007/>.
- Marullo, S., B. Buongiorno Nardelli, M. Guarracino, and R. Santoleri, 2007: Observing the mediterranean sea from space: 21 years of pathfinder-avhrr sea surface temperatures (1985 to 2005): re-analysis and validation. *Ocean Science*, **3** (2), 299–310, doi:10.5194/os-3-299-2007, URL <http://www.ocean-sci.net/3/299/2007/>.
- Milliff, R. F. and A. R. Robinson, 1992: Structure and dynamics of the rhodes gyre system and dynamical interpolation for estimates of the mesoscale variability. *Journal of Physical Oceanography*, **22** (4), 317–337, doi:10.1175/1520-0485(1992)022<0317:SADOTR>2.0.CO;2, URL [http://dx.doi.org/10.1175/1520-0485\(1992\)022<0317:SADOTR>2.0.CO;2](http://dx.doi.org/10.1175/1520-0485(1992)022<0317:SADOTR>2.0.CO;2).

- Millot, C., 1985: Some features of the algerian current. *J. Geophys. Res.*, **90 (C4)**, 7169–7176, doi:10.1029/JC090iC04p07169, URL <http://dx.doi.org/10.1029/JC090iC04p07169>.
- Molcard, A., N. Pinardi, M. Iskandarani, and D. B. Haidvogel, 2002: Wind driven general circulation of the mediterranean sea simulated with a spectral element ocean model. *Dynamics of Atmospheres and Oceans*, **35 (2)**, 97–130, URL <http://www.sciencedirect.com/science/article/pii/S037702650100080X>.
- Onken, R., A. R. Robinson, P. F. J. Lermusiaux, P. J. Haley, and L. A. Anderson, 2003: Data-driven simulations of synoptic circulation and transports in the tunisia-sardinia-sicily region. *Journal of Geophysical Research: Oceans*, **108 (C9)**, n/a–n/a, doi:10.1029/2002JC001348, URL <http://dx.doi.org/10.1029/2002JC001348>.
- Özsoy, E., et al., 1993: A synthesis of the levantine basin circulation and hydrography, 1985–1990. *Deep Sea Research Part II: Topical Studies in Oceanography*, **40 (6)**, 1075–1119, URL <http://www.sciencedirect.com/science/article/pii/096706459390063S>.
- Pedlosky, J., 1979: *Geophysical Fluid Dynamics*. 1990th ed., Springer.
- Pettenuzzo, D., W. G. Large, and N. Pinardi, 2010: On the corrections of era-40 surface flux products consistent with the mediterranean heat and water budgets and the connection between basin surface total heat flux and nao. *J. Geophys. Res.*, **115 (C6)**, doi:10.1029/2009JC005631, URL <http://dx.doi.org/10.1029/2009JC005631>.
- Pinardi, N. and G. Coppini, 2010: Operational oceanography in the mediterranean sea: the second stage of development. *Ocean Science*, **88**, 395–406.
- Pinardi, N., G. Korres, A. Lascaratos, V. Roussenov, and E. Stanev, 1997: Numerical simulation of the interannual variability of the mediterranean sea upper ocean circulation. *Geophys. Res. Lett.*, **24 (4)**, 425–428, doi:10.1029/96GL03952, URL <http://dx.doi.org/10.1029/96GL03952>.

- Pinardi, N. and E. Masetti, 2000: Variability of the large scale general circulation of the mediterranean sea from observations and modelling: a review. *Palaeogeography, Palaeoclimatology, Palaeoecology*, **158** (3-4), 153–173, URL <http://www.sciencedirect.com/science/article/pii/S0031018200000481>.
- Pinardi, N. and A. Navarra, 1993: Baroclinic wind adjustment processes in the mediterranean sea. *Deep Sea Research Part II: Topical Studies in Oceanography*, **40** (6), 1299–1326, URL <http://www.sciencedirect.com/science/article/pii/096706459390071T>.
- Pinardi, N., M. Zavatarelli, E. Arneri, A. Crise, and M. Ravaioli, 2006: The physical, sedimentary and ecological structure and variability of shelf areas in the mediterranean sea. *THE GLOBAL The global coastal ocean: interdisciplinary regional studies and syntheses*, A. Robinson and K. Brink, Eds., Harvard University Press, The Sea, Vol. 14, chap. 32.
- Pinardi, N., et al., 2003: The mediterranean ocean forecasting system: first phase of implementation (1998–2001). *Annales Geophysicae*, **21** (1), 3–20, doi:10.5194/angeo-21-3-2003, URL <http://www.ann-geophys.net/21/3/2003/>.
- Poulain, P.-M., M. Menna, and E. Mauri, 2012: Surface geostrophic circulation of the mediterranean sea derived from drifter and satellite altimeter data. *Journal of Physical Oceanography*, **42** (6), 973–990, doi:10.1175/JPO-D-11-0159.1, URL <http://dx.doi.org/10.1175/JPO-D-11-0159.1>.
- Poulain, P.-M., et al., 2007: Medargo: a drifting profiler program in the mediterranean sea. *Ocean Science*, **3** (3), 379–395, doi:10.5194/os-3-379-2007, URL <http://www.ocean-sci.net/3/379/2007/>.
- Puillat, I., R. Sorgente, A. Ribotti, S. Natale, and V. Echevin, 2006: Westward branching of liw induced by algerian anticyclonic eddies close to the sardinian slope. *Chemistry and*

- Ecology*, **22** (sup1), S293–S305, doi:10.1080/02757540600670760, URL <http://dx.doi.org/10.1080/02757540600670760>.
- Pujol, M. I. and G. Larnicol, 2005: Mediterranean sea eddy kinetic energy variability from 11 years of altimetric data. *Journal of Marine Systems*, **58** (3-4), 121–142, URL <http://www.sciencedirect.com/science/article/pii/S0924796305001442>.
- Rhines, P. B., 1979: Geostrophic turbulence. *Annual Review of Fluid Mechanics*, **11** (1), 401–441, doi:10.1146/annurev.fl.11.010179.002153, URL <http://dx.doi.org/10.1146/annurev.fl.11.010179.002153>.
- Rinaldi, E., B. Buongiorno Nardelli, E. Zambianchi, R. Santoleri, and P. M. Poulain, 2010: Lagrangian and eulerian observations of the surface circulation in the tyrrhenian sea. *J. Geophys. Res.*, **115** (C4), C04024, doi:10.1029/2009JC005535, URL <http://dx.doi.org/10.1029/2009JC005535>.
- Rixen, M., J.-M. Beckers, C. Maillard, and the MEDAR Group, 2004: A hydrographic and biochemical climatology of the mediterranean and the black sea: some statistical pitfalls. *The colour of ocean data*, V. B. E., M. Brown, M. J. Costello, C. Heip, S. Levitus, and P. Pissierssens, Eds., VLIZ Special Publication, IOC Workshop Report, 227–243, 188.
- Robinson, A. R., A. Hecht, N. Pinardi, J. Bishop, W. G. Leslie, Z. Rosentroub, A. J. Mariano, and S. Brenner, 1987: Small synoptic/mesoscale eddies and energetic variability of the eastern levantine basin. *Nature*, **327** (6118), 131–134, URL <http://dx.doi.org/10.1038/327131a0>.
- Robinson, A. R., J. Sellschopp, A. Warn-Varnas, W. G. Leslie, C. J. Lozano, P. J. Haley Jr., L. A. Anderson, and P. F. J. Lermusiaux, 1999: The atlantic ionian stream. *Journal of Marine Systems*, **20** (1–4), 129–156, URL <http://www.sciencedirect.com/science/article/pii/S0924796398000797>.

- Robinson, A. R., et al., 1991: The eastern mediterranean general circulation: features, structure and variability. *Dynamics of Atmospheres and Oceans*, **15** (3–5), 215–240, URL <http://www.sciencedirect.com/science/article/pii/0377026591900217>.
- Robinson, A. R., et al., 1992: General circulation of the eastern mediterranean. *Earth-Science Reviews*, **32** (4), 285–309, URL <http://www.sciencedirect.com/science/article/pii/001282529290002B>.
- Roether, W., B. B. Manca, B. Klein, D. Bregant, D. Georgopoulos, V. Beitzel, V. Kovačević, and A. Luchetta, 1996: Recent changes in eastern mediterranean deep waters. *Science*, **271** (5247), 333–335, doi:10.1126/science.271.5247.333, URL <http://www.sciencemag.org/content/271/5247/333.abstract>, <http://www.sciencemag.org/content/271/5247/333.full.pdf>.
- Rohling, E. and H. Bryden, 1992: Maninduced salinity and temperature increases in western mediterranean deep water. *J. Geophys. Res*, **97** (C7), 11 191–11 198.
- Smith, R., H. L. Bryden, and K. Stansfield, 2008: Observations of new western mediterranean deep water formation observations of new western mediterranean deep water formation using argo floats 2004–2006. *Ocean Science*, **4**, 133–149.
- Snaith, H. M., S. Alderson, J. Allen, and T. Guymer, 2003: Monitoring of the eastern alboran gyre using combined altimetry and in situ data. *Phil. Trans. R. Soc. Lond. A*, **361**, 65–70.
- Sparnocchia, S., G. P. Gasparini, M. Astraldi, M. Borghini, and P. Pistek, 1999: Dynamics and mixing of the eastern mediterranean outflow in the tyrrhenian basin. *Journal of Marine Systems*, **20** (1–4), 301–317, URL <http://www.sciencedirect.com/science/article/pii/S0924796398000888>.
- Struglia, M. V., A. Mariotti, and A. Filograsso, 2004: River discharge into the mediterranean sea: Climatology and aspects of the observed variability. *Journal of Climate*, **17** (24), 4740–4751, doi:10.1175/JCLI-3225.1, URL <http://dx.doi.org/10.1175/JCLI-3225.1>.

- Tonani, M., N. Pinardi, C. Fratianni, J. Pistoia, S. Dobricic, S. Pensieri, M. de Alfonso, and K. Nittis, 2009: Mediterranean forecasting system: forecast and analysis assessment through skill scores. *Ocean Science*, **5** (4), 649–660, doi:10.5194/os-5-649-2009, URL <http://www.ocean-sci.net/5/649/2009/>.
- Tsimplis, M., A. Velegrakis, P. Drakopoulos, A. Theocharis, and M. Collins, 1999: Cretan deep water outflow into the eastern mediterranean. *Progress In Oceanography*, **44** (4), 531–551, URL <http://eprints.soton.ac.uk/180303/>.
- Tziperman, E. and P. Malanotte-Rizzoli, 1991: The climatological circulation of the mediterranean sea. *Journal of Marine Research*, **49**, 411–434.
- Tziperman, E. and K. Speer, 1994: A study of water mass transformation in the mediterranean sea: analysis of climatological data and a simple three-box model. *Dynamics of Atmospheres and Oceans*, **21** (2–3), 53–82, URL <http://www.sciencedirect.com/science/article/pii/0377026594900043>.
- Vélez-Belch, P., M. Vargas-Yáñez, and J. Tintoré, 2005: Observation of a western alborán gyre migration event. *Progress In Oceanography*, **66** (2-4), 190–210, URL <http://www.sciencedirect.com/science/article/pii/S0079661105000704>.
- Wu, P., K. Haines, and P. N., 2000: Toward an understanding of deep-water renewal in the eastern mediterranean. *Journal of Physical Oceanography*, **30**, 443–458.
- Zodiatis, G., P. Drakopoulos, S. Brenner, and S. Groom, 2005: Variability of the cyprus warm core eddy during the cyclops project. *Deep Sea Research Part II: Topical Studies in Oceanography*, **52** (22–23), 2897–2910, URL <http://www.sciencedirect.com/science/article/pii/S0967064505002092>.

List of Tables

- | | | |
|---|---|----|
| 1 | Potential density thresholds for the Water Mass Formation (WMF) rate computations in each of the four regions of Fig. 1. Units are $kg\ m^{-3}$ | 36 |
| 2 | Nomenclature for the surface and intermediate depth circulation structures. | 37 |

TABLE 1. Potential density thresholds for the Water Mass Formation (WMF) rate computations in each of the four regions of Fig. 1. Units are $kg\ m^{-3}$

Areas	Water mass acronym	Density thresholds for WMF rate
1	LIW-LDW	28.95/29.10
2	CDW	29.00/29.10
3	EMDW	29.10/29.20
4	WMDW	29.00/29.10

TABLE 2. Nomenclature for the surface and intermediate depth circulation structures.

Current systems	Components
System 1	1a: Atlantic Water Current (AWC) 1b: Western and Eastern Alboran Gyres 1c: Almera-Oran front 1d: Almera-Oran cyclonic eddy 1e: Algerian Current segments 1f: Western Mid-Mediterranean Current (WMMC) 1g: Southern Sardinia Current (SCC)
System 2	2a: Gulf of Lion Gyre (GLG) 2b: Liguro-Provenal-Catalan Current (LPCC) 2c: Western Corsica Current (WCC)
System 3	3a: South-Western Tyrrhenian Gyre (SWTG) 3b: South-Eastern Tyrrhenian Gyre (SETG) 3c: Northern Tyrrhenian Gyre (NTG) 3d Middle Tyrrhenian Current 3e Eastern Corsica Current (ECC)
System 4	4a: Atlantic-Ionian Stream (AIS) 4b: Sicily Strait Tunisian Current (SSTC) 4c: Syrte Gyre (SG) 4d: Eastern Ionian Current (EIC) 4e: Pelops Gyre (PG) 4f: Northern Ionian Cyclonic Gyre
System 5	5a Eastern South-Adriatic Current (ESAC) 5b: Middle Adriatic Gyre 5c: South Adriatic Gyre 5d: Western Adriatic Coastal Current (WACC)
System 6	6a: Cretan Passage Southern Current (CPSC) 6b: Mid-Mediterranean Jet 6c: Southern Levantine Current (SLC) 6d: Mersa Matruh Gyre System (MMGS) 6e: Rhodes Gyre (RG) 6f: Shikmona Gyre System (SGS) 6g: Asia Minor Current 6h: Ierapetra Gyre (IPG) 6i: Western Cretan Cyclonic Gyre
System 7	7a: Cretan Sea Westward Current (CSWC) 7b: SouthWard Cyclades Current (SWCC) 7c: North Aegean Anticyclone

List of Figures

- 1 Mediterranean basin geometry and nomenclature for major seas and areas.
The shaded areas indicate depths less than 200 m. The four boxes (1-4) are used for the water mass formation computations. 40
- 2 The basin and time average root mean square error of misfits (difference between observations and model simulation before data insertion) for SLA (top), temperature T (bottom left) and salinity S (bottom right) panels. Units are m for SLA, $^{\circ}C$ for T and psu for S. Modified from Adani et al. (2011) 41
- 3 The 1987-2007 time-mean circulation at 15 m depth from the reanalysis: grey areas indicate velocity amplitudes greater than 0.1 ms^{-1} . 42
- 4 The 1987-2007 time-mean circulation, averaged in the layer between 200 and 300 m, from the reanalysis: grey areas indicate velocity amplitudes greater than 0.05 ms^{-1} . 43
- 5 The decadal mean circulation at 15 m depth. Upper panel: mean of Period A, 1987-1996. Bottom panel: mean of Period B, 1997-2006. Velocity amplitudes greater than 0.1 ms^{-1} are depicted by grey areas 44
- 6 The decadal mean circulation average in the 200-300 m layer. Upper panel: mean of the period 1987-1996 (Period A). Bottom panel: mean of the period 1997-2006 (Period B). Velocity amplitudes greater than 0.05 ms^{-1} are depicted by grey areas 45
- 7 The barotropic streamfunction field in Sv ($10^6 \text{ m}^3 s^{-1}$) for the 1987-2007 mean (upper panel), the 1987-1996 (middle panel) and 1997-2006 (lower panel) periods respectively. 46
- 8 Wind stress amplitude and direction (left panels) and wind stress curl (right panels) average over 1987-2007, for Period A (1987-1996) and Period B (1997-2006). Units are $N \text{ m}^{-2}$ for wind stress amplitude and $10^{-7} N \text{ m}^{-3}$ for wind stress curl 47

9	Upper panel: WMF rates (Sv) in different months for each of the four areas, average for the 21 years. Lower panel: WMF rates (Sv) for the months of February and March and for the four regions indicated in Fig. 1, as a function of time.	48
10	Yearly mean salinity below 200 metres average along the section connecting Tunisia and Sicily, shown at the upper left of the picture.	49
11	The θ/S diagram for the February-March mean profiles for all the years in the Adriatic Sea, area 3 (upper panel), and the Gulf of Lion, area 4 (lower panel). The right panels are zooms of the deep water mass characteristics for each area.	50
12	The schematic of the mean surface circulation structures as deduced from the 1987-2007 reanalysis mean flow field. Upper panel: surface circulation. Lower panel: 200-300 metres average circulation. Names of the currents are reported in Table 2	51

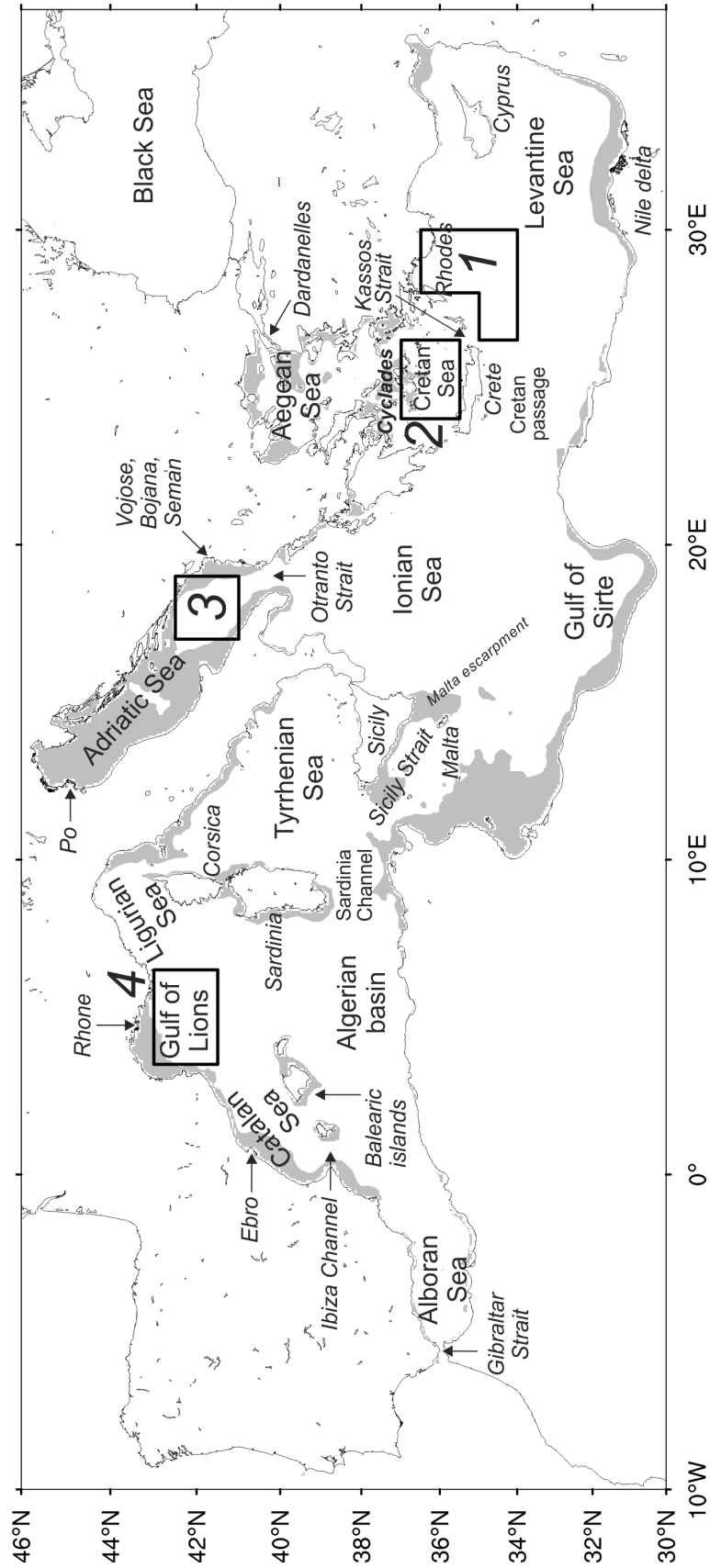


FIG. 1. Mediterranean basin geometry and nomenclature for major seas and areas. The shaded areas indicate depths less than 200 m. The four boxes (1-4) are used for the water mass formation computations.

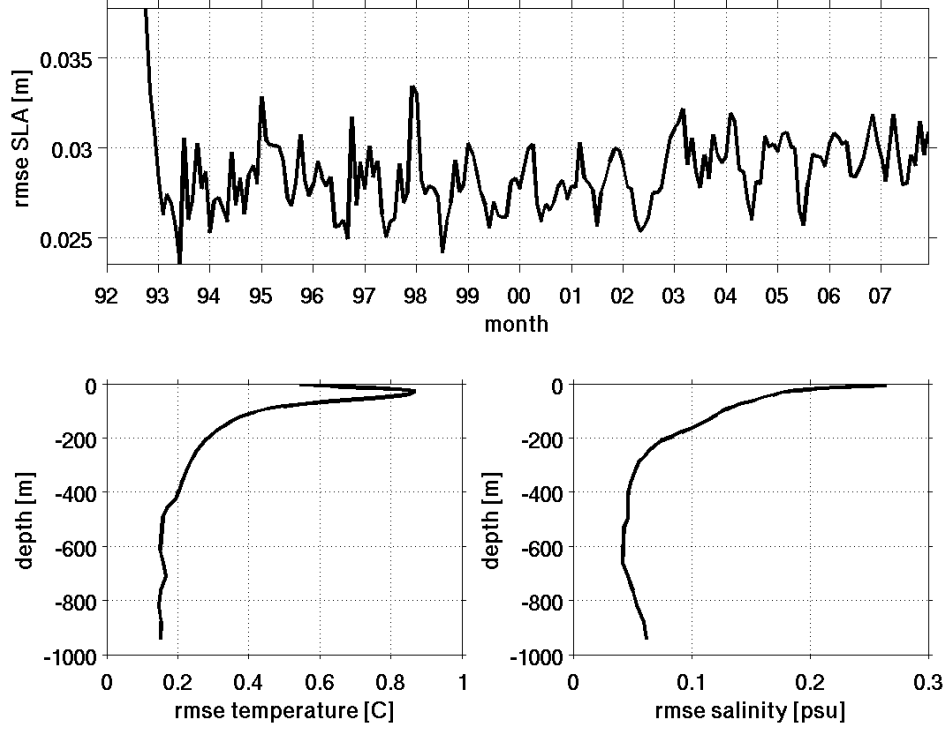


FIG. 2. The basin and time average root mean square error of misfits (difference between observations and model simulation before data insertion) for SLA (top), temperature T (bottom left) and salinity S (bottom right) panels. Units are m for SLA, $^{\circ}C$ for T and psu for S . Modified from Adani et al. (2011)

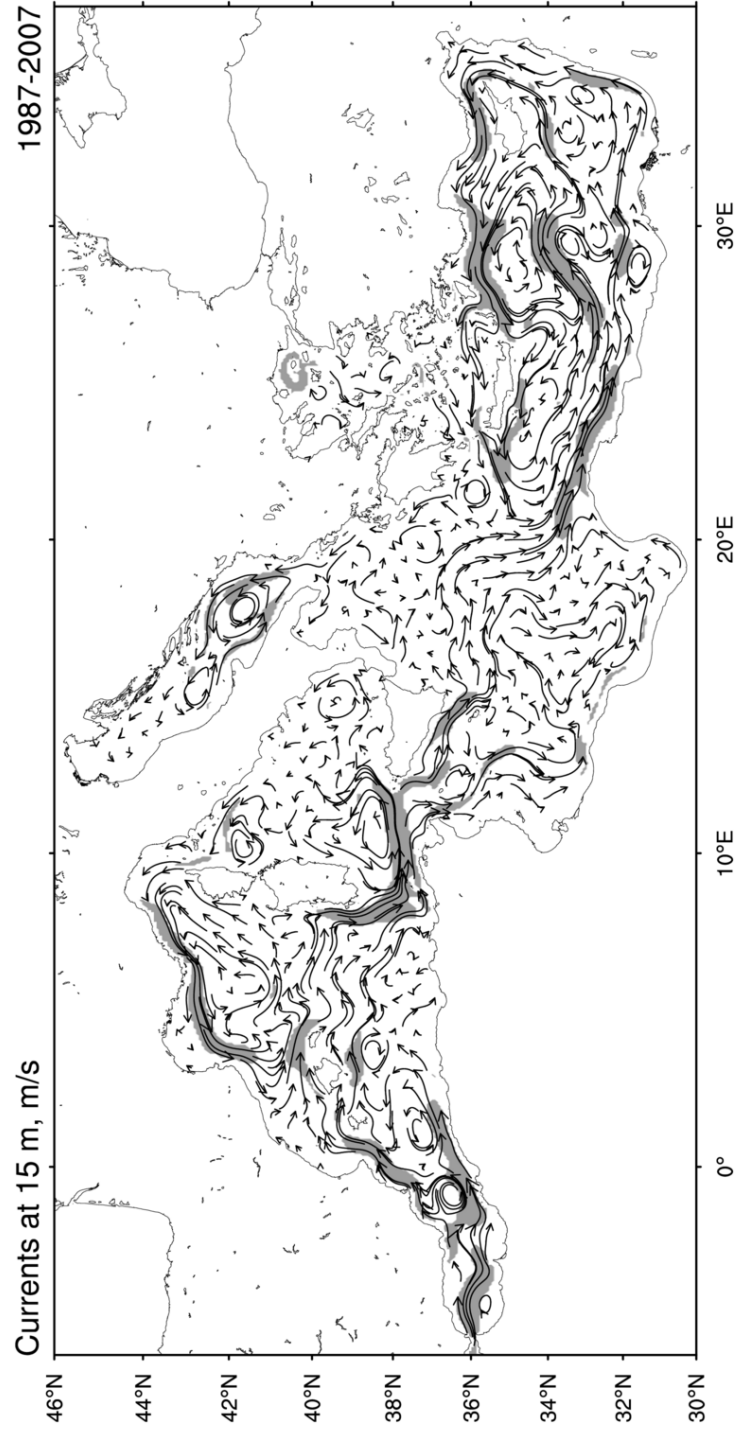


FIG. 3. The 1987-2007 time-mean circulation at 15 m depth from the reanalysis: grey areas indicate velocity amplitudes greater than 0.1 m s^{-1} .

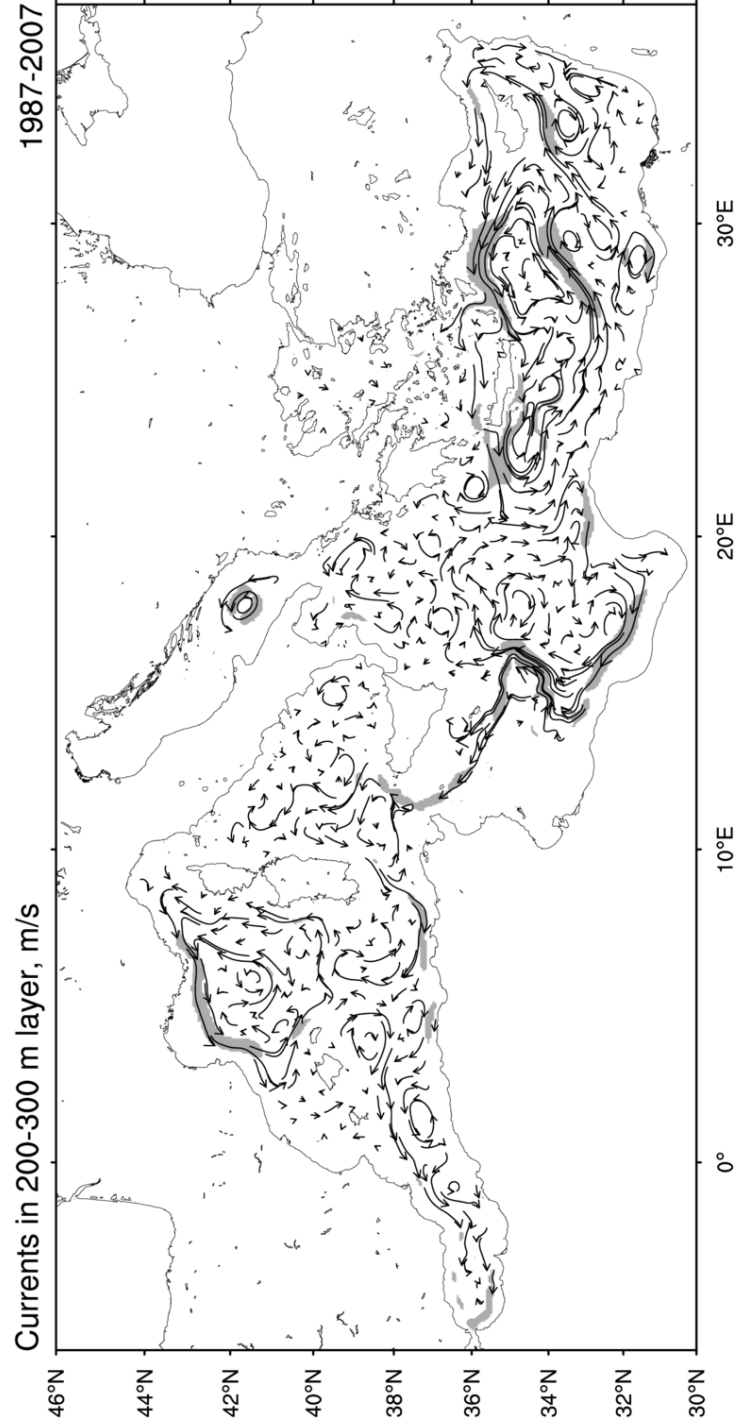


FIG. 4. The 1987-2007 time-mean circulation, averaged in the layer between 200 and 300 m, from the reanalysis: grey areas indicate velocity amplitudes greater than 0.05 m s^{-1} .

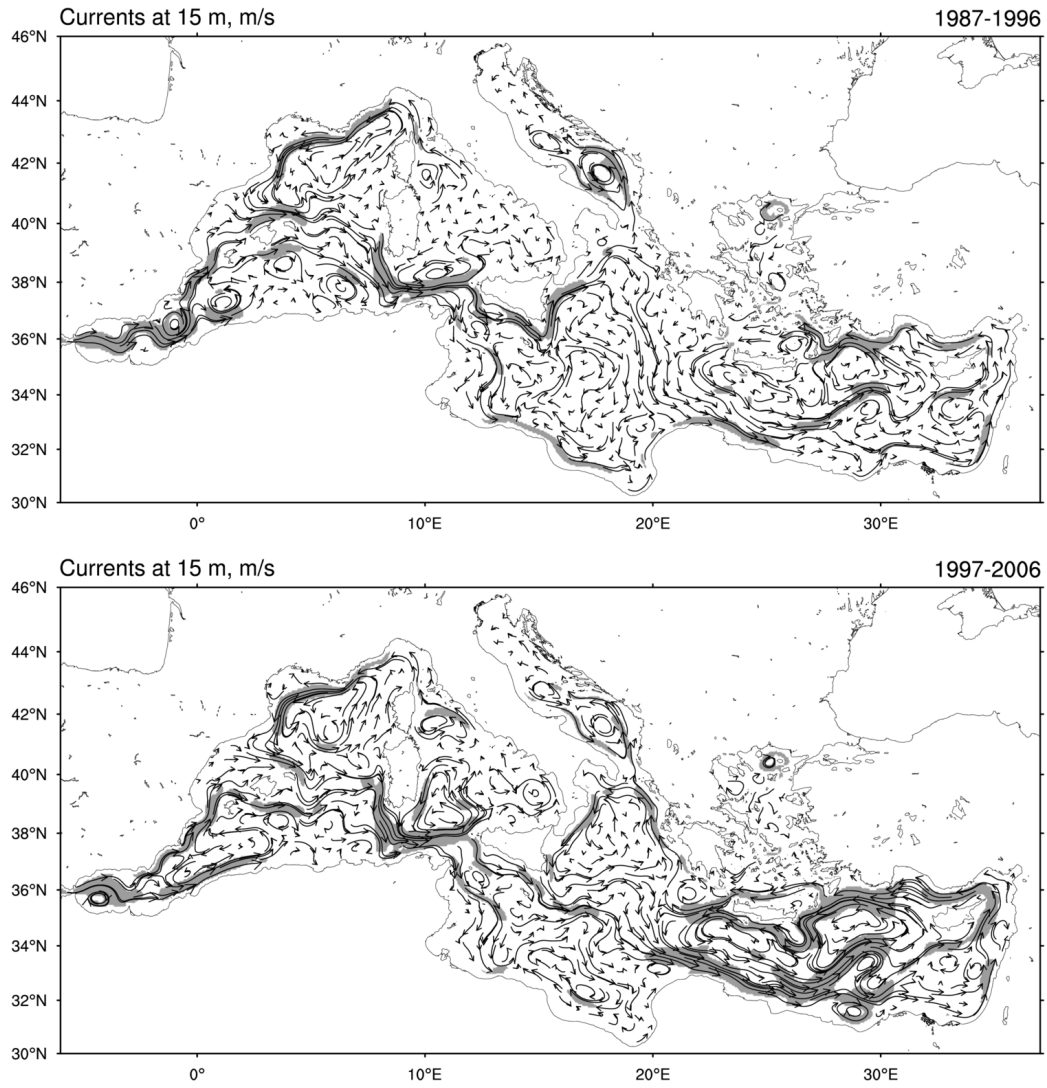


FIG. 5. The decadal mean circulation at 15 m depth. Upper panel: mean of Period A, 1987-1996. Bottom panel: mean of Period B, 1997-2006. Velocity amplitudes greater than 0.1 m/s are depicted by grey areas

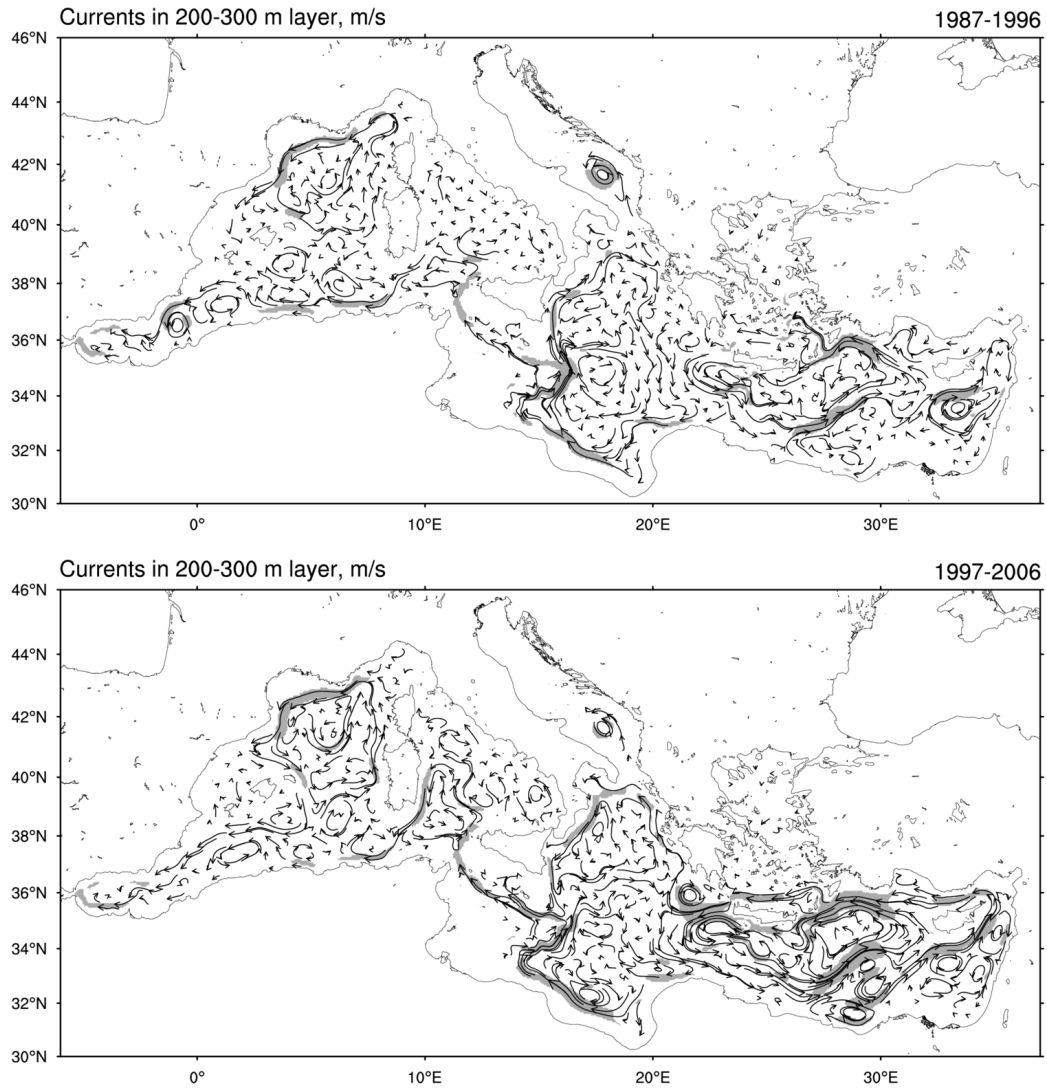


FIG. 6. The decadal mean circulation average in the 200-300 m layer. Upper panel: mean of the period 1987-1996 (Period A). Bottom panel: mean of the period 1997-2006 (Period B). Velocity amplitudes greater than 0.05 m s^{-1} are depicted by grey areas

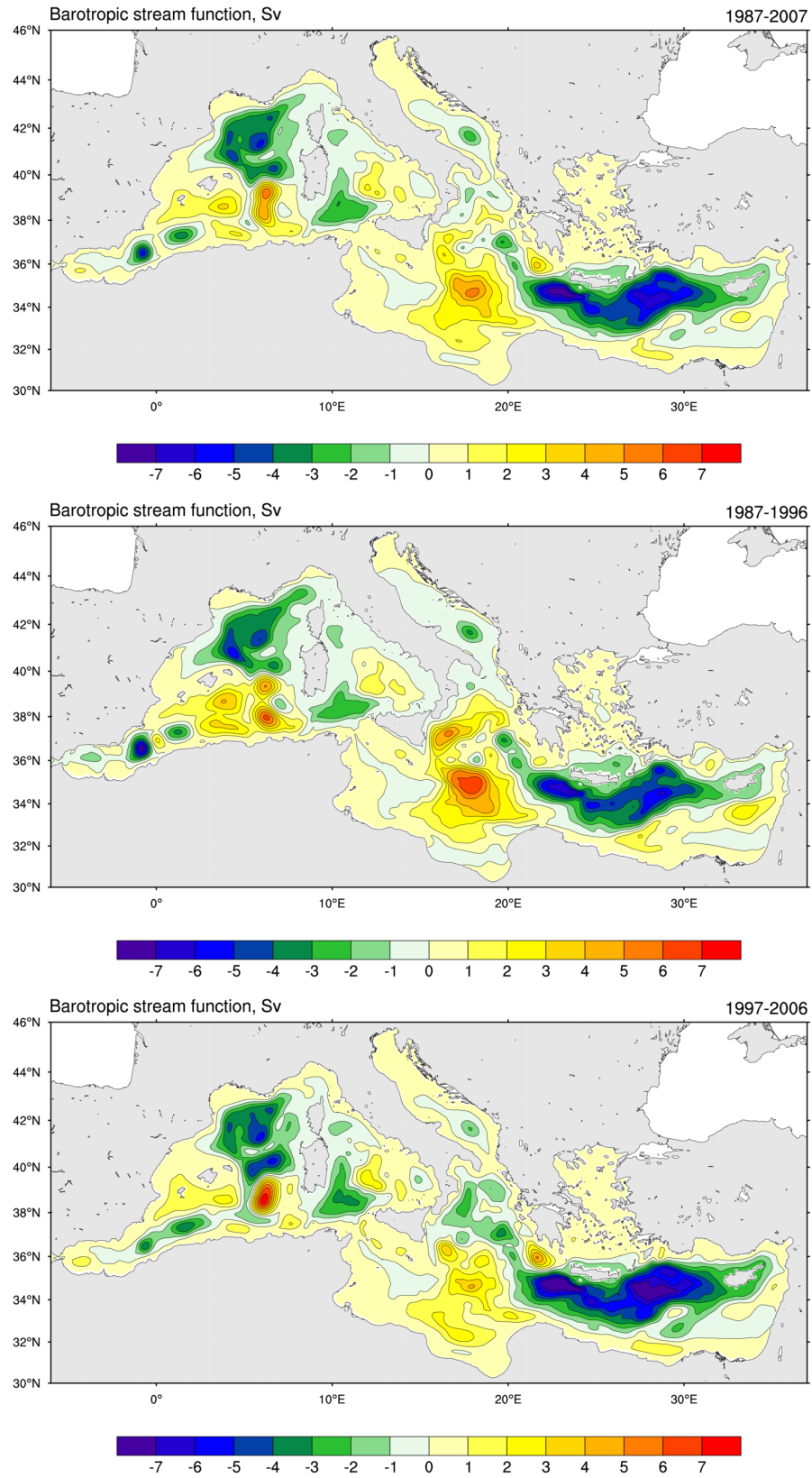


FIG. 7. The barotropic streamfunction field in Sv ($10^6 m^3 s^{-1}$) for the 1987-2007 mean (upper panel), the 1987-1996 (middle panel) and 1997-2006 (lower panel) periods respectively.

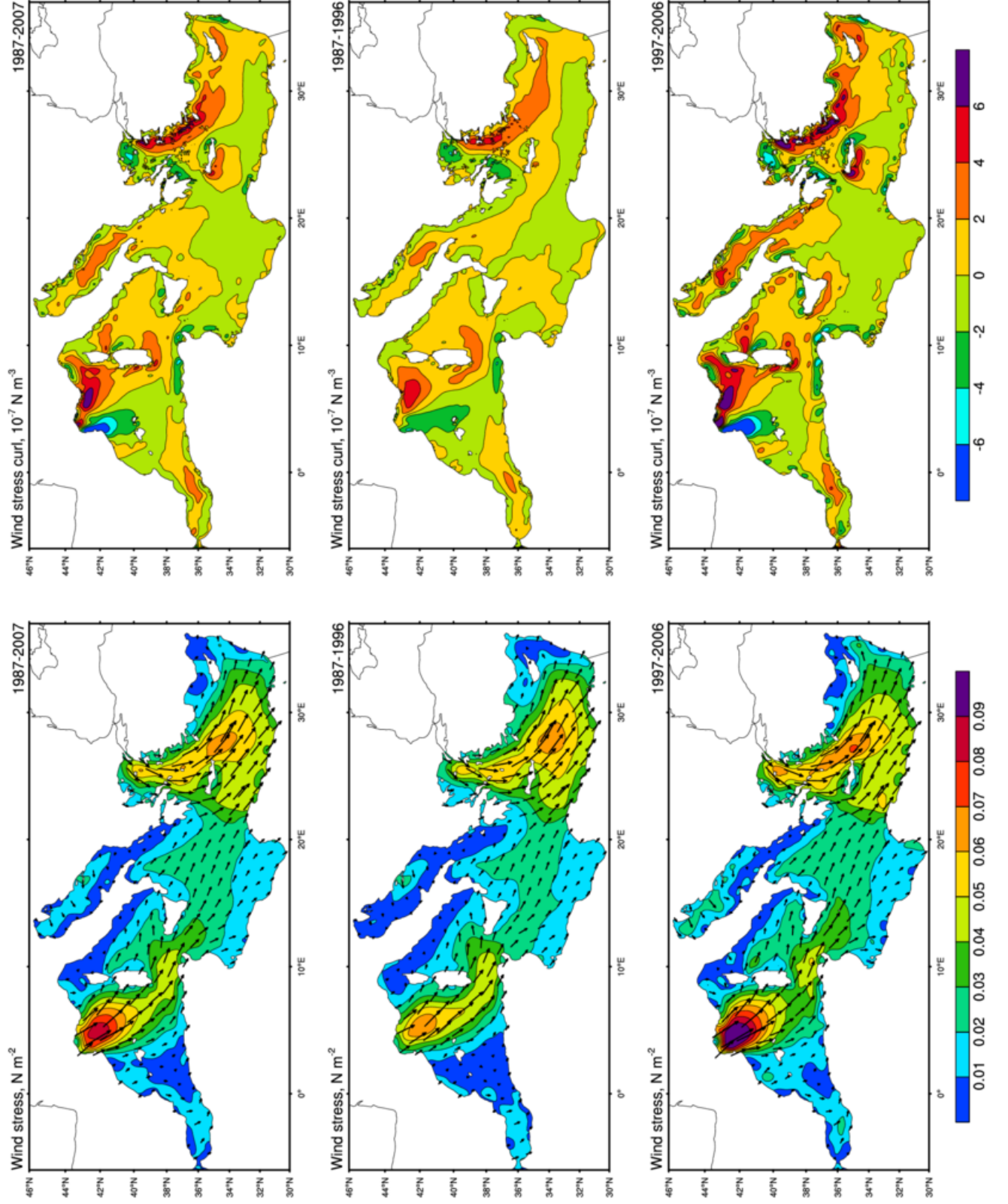


FIG. 8. Wind stress amplitude and direction (left panels) and wind stress curl (right panels) average over 1987-2007, for Period A (1987-1996) and Period B (1997-2006). Units are $N m^{-2}$ for wind stress amplitude and $10^{-7} N m^{-3}$ for wind stress curl

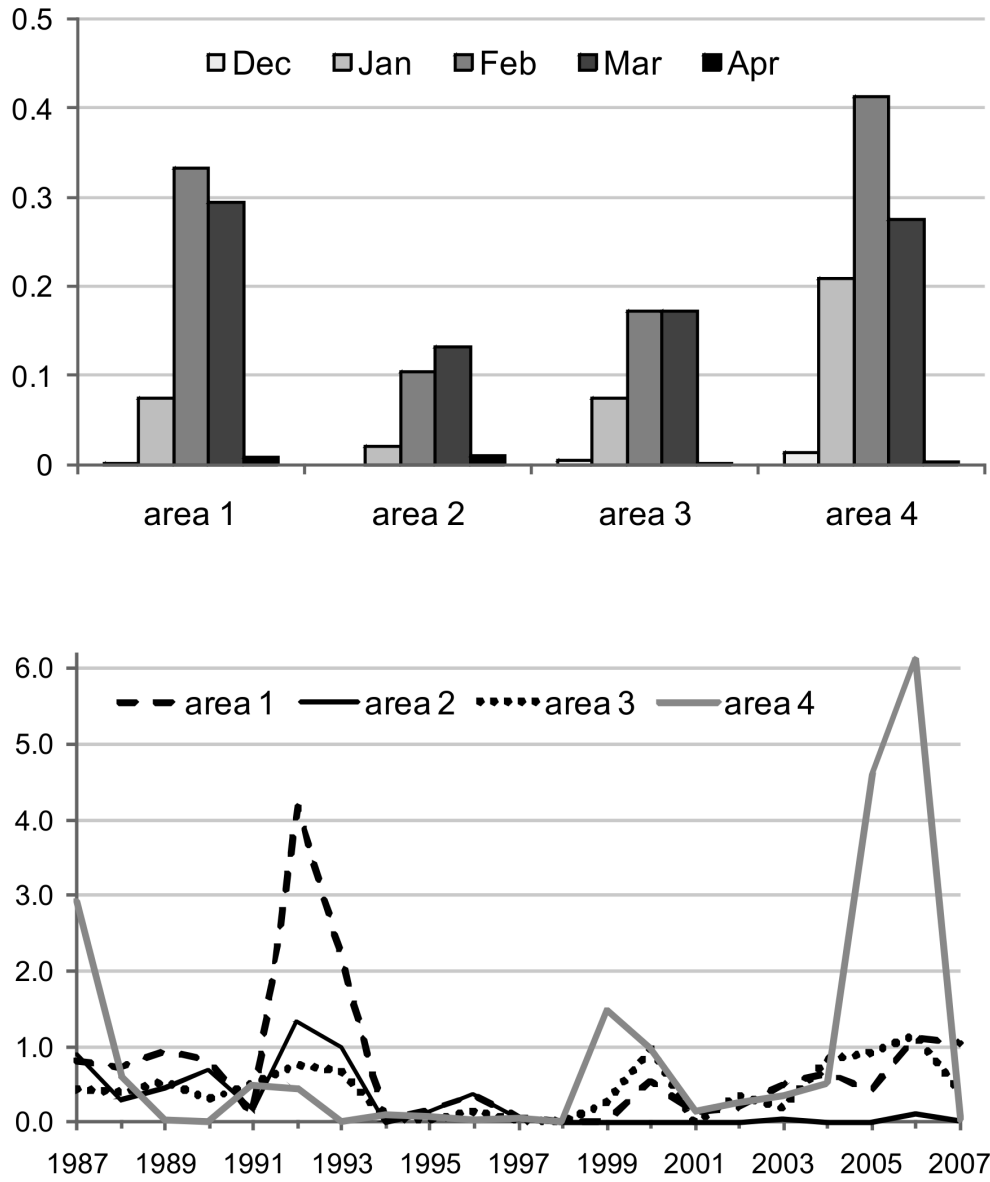


FIG. 9. Upper panel: WMF rates (Sv) in different months for each of the four areas, average for the 21 years. Lower panel: WMF rates (Sv) for the months of February and March and for the four regions indicated in Fig. 1, as a function of time.

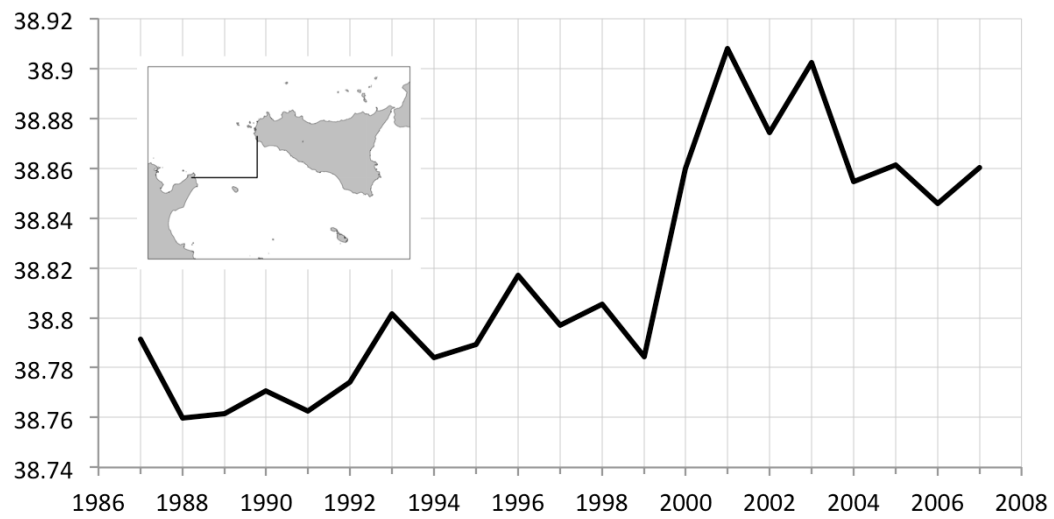


FIG. 10. Yearly mean salinity below 200 metres average along the section connecting Tunisia and Sicily, shown at the upper left of the picture.

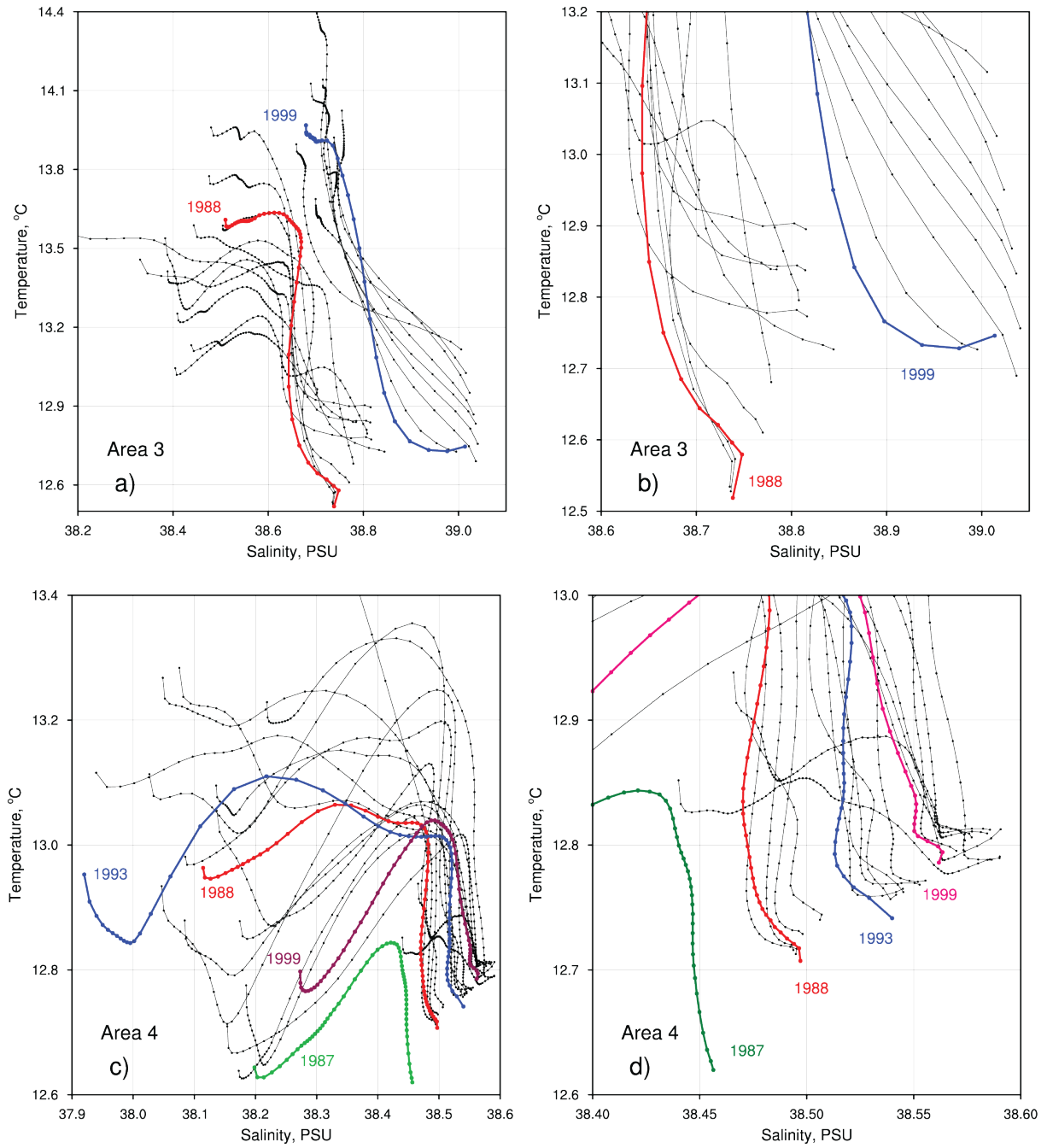


FIG. 11. The θ/S diagram for the February-March mean profiles for all the years in the Adriatic Sea, area 3 (upper panel), and the Gulf of Lion, area 4 (lower panel). The right panels are zooms of the deep water mass characteristics for each area.

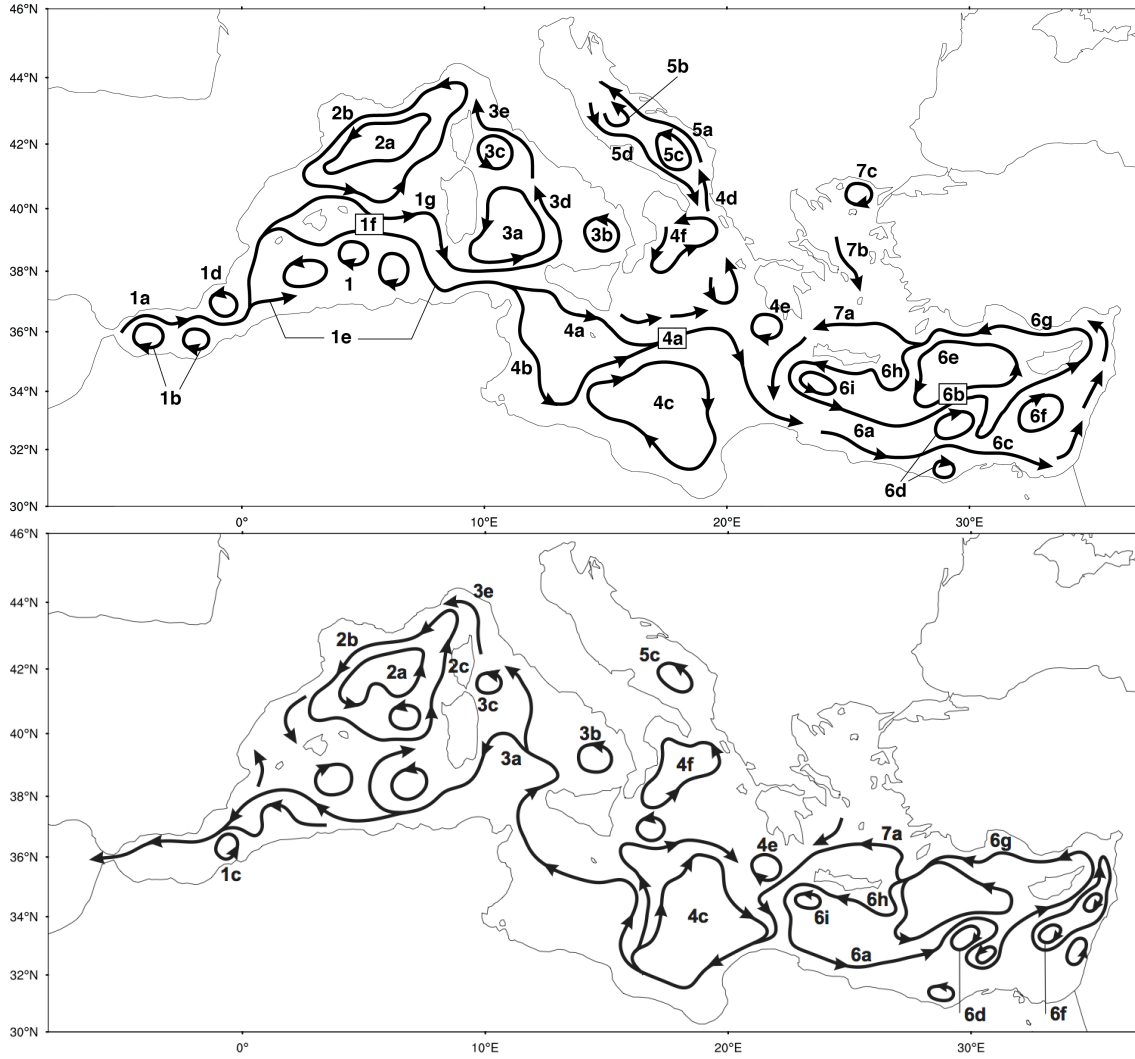


FIG. 12. The schematic of the mean surface circulation structures as deduced from the 1987-2007 reanalysis mean flow field. Upper panel: surface circulation. Lower panel: 200-300 metres average circulation. Names of the currents are reported in Table 2